



**HAL**  
open science

## Validation of a novel immersive Virtual Reality setup with responses of wild-caught freely-moving coral reef fish

Manuel Vidal, Suzanne Mills, Emma Gairin, Frédéric Bertucci, David Lecchini

### ► To cite this version:

Manuel Vidal, Suzanne Mills, Emma Gairin, Frédéric Bertucci, David Lecchini. Validation of a novel immersive Virtual Reality setup with responses of wild-caught freely-moving coral reef fish. *Animal Behaviour*, In press, 10.1101/2022.11.01.514726 . hal-04239926

**HAL Id: hal-04239926**

**<https://hal.science/hal-04239926v1>**

Submitted on 12 Oct 2023

**HAL** is a multi-disciplinary open access archive for the deposit and dissemination of scientific research documents, whether they are published or not. The documents may come from teaching and research institutions in France or abroad, or from public or private research centers.

L'archive ouverte pluridisciplinaire **HAL**, est destinée au dépôt et à la diffusion de documents scientifiques de niveau recherche, publiés ou non, émanant des établissements d'enseignement et de recherche français ou étrangers, des laboratoires publics ou privés.

# Validation of a novel immersive Virtual Reality setup with responses of wild-caught freely-moving coral reef fish

Manuel Vidal<sup>a,\*</sup>, Suzanne C. Mills<sup>b,e</sup>, Emma Gairin<sup>c</sup>, Frédéric Bertucci<sup>b,d</sup>, and David Lecchini<sup>b,e</sup>

a Institut de Neurosciences de la Timone, UMR 7289, Aix-Marseille Université, CNRS, Marseille, France

b PSL Université Paris, EPHE-UPVD-CNRS, UAR3278 CRIOBE, Moorea, French Polynesia

c Marine Eco-Evo-Devo Unit, Okinawa Institute of Science and Technology, Okinawa, Japan

d Marbec, CNRS-IRD-IFREMER-INRAE-University of Montpellier, Sète, France

e Laboratoire d'Excellence "CORAIL", France

\* Corresponding author: [manuel.vidal@univ-amu.fr](mailto:manuel.vidal@univ-amu.fr)

## Abstract

Virtual Reality (VR) enables standardised stimuli to invoke behavioural responses in animals, however, in fish studies VR has been limited to either basic virtual stimulation projected below the bowl for freely-swimming individuals or a simple virtual arena rendered over a large field-of-view for head-restrained individuals. We developed a novel immersive VR setup with real-time rendering of animated 3D scenarios, validated in a proof of concept study on the behaviour of coral reef post-larval fish. Fish use a variety of cues to select a habitat during the recruitment stage, and to recognize conspecifics and predators, but which visual cues are used remains unknown. We measured behavioural responses of groups of five convict surgeonfish (*Acanthurus triostegus*) to simulations of habitats, static or moving shoals of conspecifics, predators, and non-aggressive heterospecifics. Post-larval fish were consistently attracted to virtual corals and conspecifics presented statically, but repulsed by their predators (bluefin jacks, *Caranx melampygus*). When simulated shoals passed nearby repeatedly, they were again attracted by conspecifics showing a tendency to follow the shoal, whereas they moved repeatedly to the back of the passing predator shoal. They also discriminated between species of similar sizes: they were attracted more to conspecifics than butterflyfish (*Forcipiger longirostris*), and repulsed more by predators than parrotfish (*Scarus psittacus*). The quality of visual simulations was high enough to identify between visual cues – size, body shape, colour pattern – used by post-larval fish in species recognition. Despite a tracking technology limited to fish 2D positions in the aquarium, preventing the real-time updating of the rendered viewpoint, we could show that VR and modern tracking technologies offer new possibilities to investigate fish behaviour through the quantitative analysis of their physical reactions to highly-controlled scenarios.

**Keywords.** Virtual Reality; proof of concept; post-larval; reef fish; visual recognition; conspecific; predator; habitat; recruitment

## 35 Introduction

36 Animal behaviours such as foraging, habitat choice, predator avoidance, social behaviour and  
37 mate choice, are studied for multiple reasons including to understand how they have been shaped by  
38 natural selection or how they are impacted by internal and external stimuli. Animal behavioural  
39 studies face two challenges: one is related to the subject's own understanding of the task to be  
40 performed, and the other is linked to measuring its response (Drew, 2019). One way to solve the first  
41 challenge is to use a task that requires a natural reaction to a stimulation presented in an ecological  
42 context, and for which the understanding is implicit. Conventional experimental approaches used live  
43 stimulus animals or environments, but they suffered from a lack of control and standardization as  
44 neither the behaviour of stimulus animals nor the local environment can be completely controlled.  
45 For instance, testing behavioural dominance in response to an opponent requires trials with multiple  
46 opponents of known dominance and applying a correction factor (Alatalo et al., 1991; Mills et al.,  
47 2007). Furthermore, experiments with live stimulus animals often require long methodological  
48 preparation, which limits the number of possible manipulations (Neri, 2012). As a result, stimuli have  
49 been artificially designed to provide repeatable behavioural observations (Carmichael, 1952) and  
50 have evolved from simple pictures and physical models to Virtual Reality (VR) that enables  
51 standardised manipulations of stimulus behaviours or environments. The second challenge, response  
52 measurement, has been solved using video-based tracking systems of freely moving focal animals,  
53 which assumes that the behavioural response lies in the kinematics of the animal, e.g. position,  
54 orientation, speed, spatial dispersion. Therefore VR provides a good methodological compromise  
55 between a perfectly controlled but not ecologically valid stimulation, and a realistic natural situation  
56 with little to no parameter control. Although VR simulators have been widely used over the last 25  
57 years to elucidate the perceptual, sensorimotor and cognitive mechanisms underlying human spatial  
58 orientation in the environment (e.g. Tarr & Warren, 2002; Vidal et al., 2004; Mossio et al., 2008; Vidal  
59 et al., 2009; Vidal & Bühlhoff, 2009), only recently have they been adapted to investigate animal  
60 behaviour, ranging from mice to fruit flies and zebrafish (Harvey et al., 2009; Stowers et al., 2017; for  
61 a discussion, see Drew, 2019).

62 The first studies of fish visual behaviour that used pre-recorded video stimuli in mating  
63 preference tasks date from the end of the nineties, with either manipulated real-videos for  
64 (Rosenthal & Evans, 1998) or synthetically generated videos of 3D animated fish (Künzler & Bakker,  
65 1998). Ten years later, the same team showed that computer animations of artificial fish allow  
66 manipulating movement, body shape and skin-colour to investigate preferences in the cichlid  
67 *Pelvicachromis taeniatus* (Baldauf et al., 2009). The survival potential of prey group formation and  
68 movement was measured through the response of real predatory bluegill sunfish (*Lepomis*  
69 *macrochirus*) to virtual prey projections (Ioannou et al., 2012). Both experiments used one or two

70 screen monitors to display the virtual images. Since then, technology has greatly improved, and VR  
71 has led to considerable advances in the understanding of the neural bases of zebrafish visual  
72 behaviour (Portugues & Engert, 2009; Dunn et al., 2016), shoaling behaviour and social interactions  
73 (Larsch & Baier, 2018; Huang et al., 2020; Harpaz et al., 2021), as well as decision making (Barker &  
74 Baier, 2015). However, to date the use of VR to study fish behaviour has been restricted to zebrafish  
75 larvae, either moving freely in a bowl responding to basic virtual stimulation projected below such as  
76 moving dark disks, a checker board or grass bottom, coupled with infrared 3D tracking (Stowers et  
77 al., 2017), or with head-restrained zebrafish responding to conspecifics in a simple virtual arena  
78 covering 180° of the visual field and rotating based on tail movements (Huang et al., 2020).  
79 Therefore, modern VR technology including realistic rendering and immersion in a large 3D volume  
80 has not been adapted to fish studies yet, despite the limitless number of findings that can be  
81 generated in terms of quantitative animal behaviour and their ecological implications. Here, we carry  
82 out a proof of concept study on a new setup for freely-moving fish within an aquarium with an  
83 immersive full-field rendering of virtual scenes using projections not only from below, but on all five  
84 sides (except the top). We propose that our VR setup has considerable future potential for all types  
85 of behavioural studies on fish species at any stage of their life-cycle. Here, our methodology is tested  
86 on the behaviour of post-larval coral reef fish exposed to multiple scenarios during their recruitment.

87 In all marine environments, one of the main mysteries of fish ecology is how larvae recruit  
88 onto the relatively rare patches of coastal habitats (for review, see Doherty, 2002; Barth et al., 2015).  
89 The life-cycle of most reef fish species starts with a planktonic larval phase, lasting several weeks,  
90 followed by recruitment and a sedentary reef phase for juveniles and adults (Leis & McCormick,  
91 2002). At the end of the pelagic phase, this recruitment relies on the detection of a suitable habitat  
92 which will facilitate larval survival and growth (Doherty, 2002; Lecchini & Galzin, 2003). Simultaneous  
93 to that choice, species-specific changes in morphology and physiology, metamorphosis, occur. These  
94 changes are linked to ecological shifts with modifications of diet and diel activity period (McCormick  
95 et al., 2002; Besson et al., 2017; Holzer et al., 2017) but also of the sensory systems (Lecchini et al.,  
96 2005; Tettamanti et al., 2019). Many studies have highlighted the role of sensory and swimming  
97 mechanisms in larval habitat selection, most focusing on the role of chemical (e.g. Atema et al., 2002;  
98 Vail & McCormick, 2011; Coppock et al., 2013; Lecchini et al., 2013) and acoustic cues (e.g. Tolimieri  
99 et al., 2004; Montgomery et al., 2006; Holles et al., 2013; Parmentier et al., 2015). However, vision is  
100 a well-developed sense in coral reef fish larvae (Myrberg & Fuiman, 2002), effective to up to 10 m for  
101 *Plectropomus leopardus* post-larval fish at recruitment (Leis & Carson-Ewart, 1999). Once larvae are  
102 close to a reef, visual cues of conspecifics become important in the recruitment process (Booth,  
103 1992; Barth et al., 2015). However, only a few studies have identified the visual parameters used by  
104 larvae to recognize conspecifics or predators (e.g. Leis & Carson-Ewart, 1999; Booth, 1992; Huijbers  
105 et al., 2012; Lecchini et al., 2014). To test how post-larval fish (i.e., larvae having recruited onto a

106 habitat, with metamorphosis still on-going; see Besson et al., 2020) interpret a range of sensory cues,  
107 behavioural experiments can reproduce and control a large variety of combinations of visual cues  
108 (Barth et al., 2015). VR is potentially an excellent method to test such behaviours as visual factors  
109 such as size, colour patterns, and the behaviour of other individuals can be tightly controlled  
110 (Stowers et al., 2017; Brookes et al., 2020). Here, we experimentally validate a new and fully  
111 immersive VR setup for fish by testing several presentation scenarios, named trials, in three  
112 experiments on post-larval fish during recruitment.

113 We used an innovative immersive VR setup to understand how post-larval convict  
114 surgeonfish (*Acanthurus triostegus*) visually recognize a suitable habitat, adult conspecifics and one  
115 of their predators (bluefin jacks, *Caranx melampygus*). Our first objective was to experimentally  
116 validate the use of simulated 3D models of fishes in a VR setup by confirming that they are realistic  
117 enough to cause natural reactions in post-larval fish. Three main experiments were carried out to  
118 identify the visual cues used by *A. triostegus* post-larvae to recognize adult conspecifics and a  
119 predator. Trials included the presentation of virtual habitats and virtual monospecific fish shoals of  
120 conspecifics or predators. The trials with virtual fish species were projected either static (moving in  
121 place, Experiments 1 and 2) or dynamic (swimming past on one side of the aquarium, Experiments 2  
122 and 3) and a coral reef habitat on all other sides, aimed to virtually reproduce previous studies in  
123 which the reaction to either static fish in the corners of the aquarium (Katzir, 1981) or to real fish  
124 swimming in a separate adjacent aquarium (Roux et al., 2016) had been studied. We also tested  
125 post-larval behavioural responses to two virtual fish shoals swimming past on either side of the  
126 aquarium, each with different species, inducing a forced choice (Experiment 3). Furthermore, this  
127 experiment was designed to test whether post-larvae can discriminate between the size and species  
128 of virtual fish, *i.e.*, if post-larval fish consider larger virtual fish as threats irrespective of species. The  
129 advantage of our virtual presentation compared to using live stimuli, is that we were able to measure  
130 post-larval fish behaviour rapidly in response to different trials. Our second objective was to validate  
131 the automation of post-larval fish position tracking within the test aquarium at high temporal  
132 resolution, enabling detailed characterization of their behavioural responses to each scenario.

## 133 The Immersive VR Setup

134 The experimental setup was composed of three connected modules: the focal aquarium in  
135 which post-larvae could swim freely suspended inside the test aquarium, the rendering module  
136 which projected the interactive 3D virtual environments depicting a subaquatic natural scene with  
137 fishes and corals, and the tracking module which recorded post-larval behaviour in real-time. The  
138 software was developed in the lab and the hardware was assembled by Immersion™.

## 139 Test and focal aquaria

140 The test aquarium was a rectangular prism made of 10 mm-thick Plexiglas plates, with a  
141 50×50-cm square bottom and 35 cm-high lateral sides. The external faces of the bottom and lateral  
142 sides were covered by a retro projection translucent, but not transparent, film, as such post-larval  
143 fish inside the aquarium could not see the room surrounding the setup, except for the ceiling. The  
144 aquarium was filled with 78 litres of sea water so that the water surface was aligned with the upper  
145 limit of the video projection. The entire setup was mounted on a structure made of 4-cm squared-  
146 section aluminium bars (**Figure 1A**). A smaller focal aquarium (dimensions 20×20×20 cm) in which the  
147 post-larvae were placed, was attached to the structure using chains and positioned inside the test  
148 aquarium (**Figure 1B**). This smaller focal aquarium limited post-larval movement maintaining them  
149 within the range where geometrical projection distortion and image corrections were minimal and  
150 would not affect post-larval behaviour (see Video-based tracking section).

## 151 Virtual scene rendering

152 Five video projectors ensured an immersive full-field rendering of the virtual scenes on five  
153 sides of the test aquarium (Optoma ML1050ST+, running at 60Hz with a resolution of 1280×800 for  
154 the side views and 800×800 for the bottom view). The visible range of post-larval *A. triostegus* likely  
155 falls within the human visible range, enabling the use of these video projectors for visual stimulation  
156 (Losey et al., 2003). The baseline 3D virtual environment, which was projected on all five aquarium  
157 sides at all times, consisted of a sandy bottom at 2 m, with simulated surface ripples and caustics  
158 projected on the ground. The virtual viewpoint (position of rendering cameras), which defines the  
159 physical-to-virtual relationship, was placed at a depth of 0.75 cm and corresponded to the centre of  
160 the test aquarium. Different scenarios (trials) consisting of coral pinnacles (healthy or bleached) as  
161 well as animated fish of various species were added to the baseline 3D environment, depending on  
162 the simulation, on the left or right side of the aquarium, at a distance of 50 cm. Simulated shoals of  
163 five fish could either swim in place on either side or follow a tangent trajectory at a given speed. We  
164 used Epic Games Unreal™ Engine 4.23 to render the virtual fish and scene according to the desired

165 test conditions, and to manage the sequencing of trial executions. **Figure 2A** shows how three live  
166 post-larvae view a virtual scene of corals and adult surgeonfish from within their focal aquarium.

## 167 **Video-based tracking**

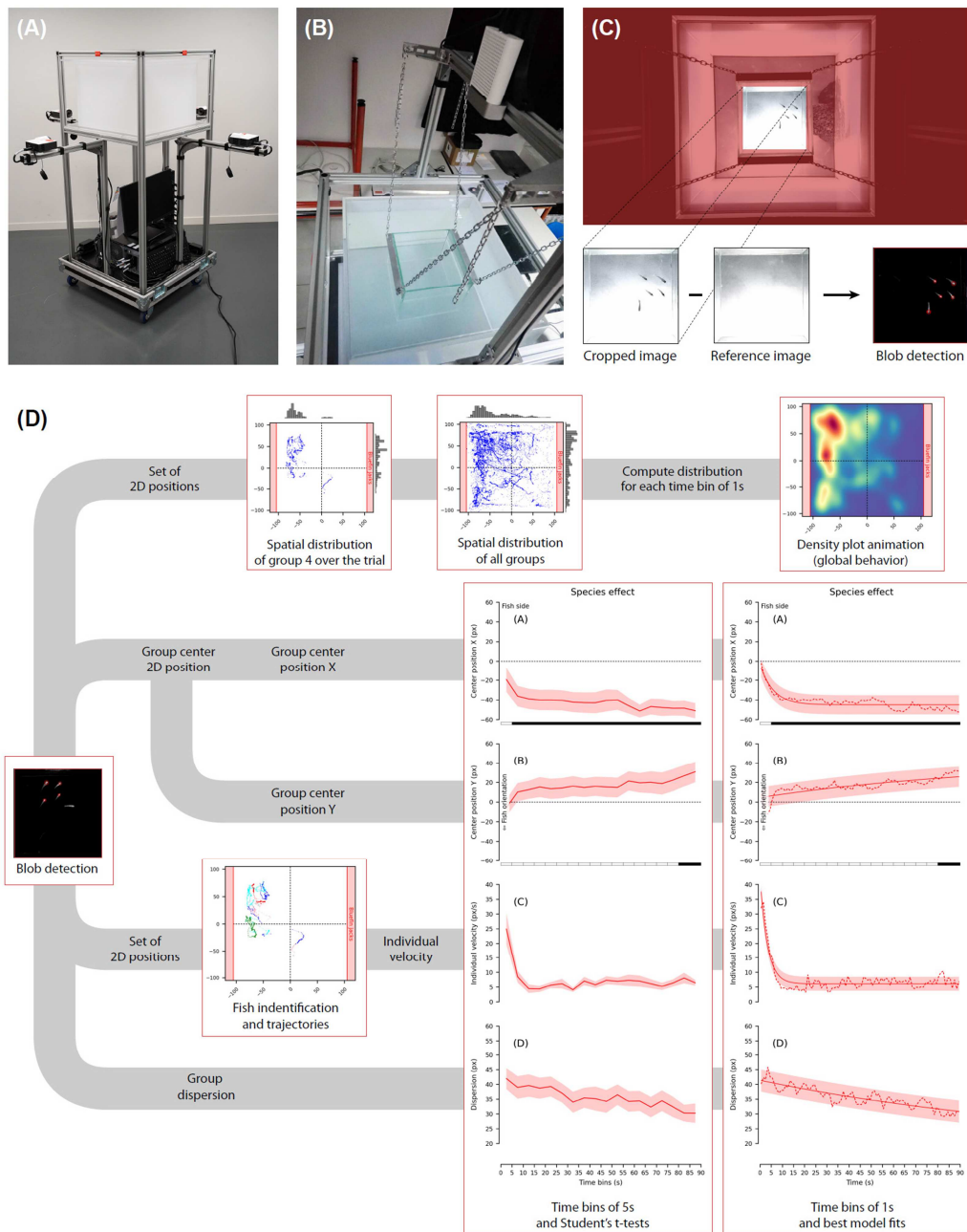
168 A Microsoft™ Kinect Azure depth camera was placed 50 cm above the water surface to  
169 continuously monitor post-larval fish behaviour in the focal aquarium (**Figure 1B**). For each trial, a  
170 top-view colour video was recorded and processed in real-time at a frequency of 5Hz to compute the  
171 2D location of each post-larval fish. In the original design of the setup, we planned to track real-time  
172 3D positions of fish with the infra-red (IR) sensor of the Microsoft Azure Kinect depth camera.  
173 However, this technology revealed not suitable for underwater tracking due to the large hot-spot  
174 created on the surface of the water by the IR grid-spot. For this reason, we switched to the color  
175 sensor and could not adjust in real-time the rendering viewpoint according to fish position in the  
176 aquarium. The detection pipeline used both the OpenCV image processing library and the Kinect  
177 Azure SDK (**Figure 1C**). Images were extracted from the colour video stream and cropped. The  
178 constant background was then removed by subtracting a reference image captured before placing  
179 fish in the aquarium. The 2D location of each fish was detected using the OpenCV blob detector with  
180 parameters adjusted appropriately. The computer performing the virtual rendering also executed  
181 this processing pipeline in real-time. The processing had no impact on the frame rate of the visual  
182 scene. Tracking performance is provided in Appendix **Fig A1**.

## 183 **Tracking post-processing**

184 The 2D positions of each post-larval fish in groups of 5 were detected at a sampling rate of  
185 5Hz. This automated process is not error-free: in some frames, fewer than five blobs were detected  
186 (low signal for smaller juveniles swimming at greater depth or due to overlaps) or more than five  
187 blobs (fish reflecting on the Plexiglas when swimming close to the aquarium sides). The tracking post-  
188 processing pipeline using Python scripts involved seven steps (**Figure 1D**). First, frames for which only  
189 one or two fish were detected were removed to reduce group mean value noise. Second, reflection  
190 biases mentioned above were limited by removing the outermost blob when a pair of fish and wall-  
191 reflected fish was potentially detected (*i.e.*, when two vertically- or horizontally-aligned blobs were  
192 very close to each other and to the edge of the aquarium). Third, as the automated detection cannot  
193 identify and track individual fish from one frame to the next (identification problem), a minimal  
194 heuristic distance was used to track the fish. This distance was only used when the position change  
195 of a blob from one frame to the next was minimal (with five individuals, there were 120 possible  
196 combinations across each pair of frames). This provided the (partial) trajectories and instantaneous  
197 velocities of each individual. Transiently missing or extra blobs could produce artificial jumps to  
198 distant locations; above a given distance threshold between frames (corresponding to 15cm/s) these

199 jumps were ignored in the computation of individual instantaneous velocities. The trajectory  
200 reconstructions are plotted with coloured lines for each tracked fish in a (X, Y) square graph  
201 representing the aquarium. Fourth, for each validated frame, the X and Y position of the centre of  
202 the group, the dispersion relative to the centre (mean distance to the centre), and average individual  
203 velocities were computed. To account for the fact that the stimulations were presented either on the  
204 right or the left, the sign of the X coordinates was inverted when the stimulation was presented on  
205 the left. Fifth, in order to visualize the raw results for each experiment and each tested condition, 2D  
206 scatterplots with all valid fish positions from all groups, and normalized X- and Y-position distribution  
207 histograms (with 5-pixel large bins) are used (representative scatterplot from Experiment 1 is in **Fig**  
208 **A3**). Sixth, in order to visualize the average behavioural responses across time for each experiment  
209 and tested condition, heatmaps of fish position density in the aquarium were plotted in successive 1-  
210 second intervals. Lastly, the time-series for each of the four behavioural measures (group centre X-  
211 and Y-position, dispersion and individual velocities) were binned into 5-second intervals for the  
212 statistical tests, and into 1-second intervals to find the best behavioural model fit.





213

214

215

216

217

218

219

220

221

222

223

224

225

226

**Figure 1.** (A) View of the experimental setup as delivered by Immersion™ with the test aquarium (dimensions 50×50×35 cm) and 5 video projectors (four lateral sides plus bottom). (B) View of the smaller focal aquarium (20×20×20 cm) placed inside the test aquarium in order to limit the displacement range of fish, and of the Microsoft™ Kinect Azure camera recording the behavioural responses. (C) Illustration of the detection pipeline starting from the camera view to blob detection executed after cropping and subtracting the reference image, followed by the tracking post-processing pipeline (D). Detected 2D positions were used to characterize post-larvae behavioural responses. For each condition, the overall behaviour obtained combining data from all tested groups is visible in the animation of the 2D density heat maps generated every second. The X and Y positions of the centre of the groups, the individual velocities and the dispersions were averaged across time-bins of 5s to perform statistical comparisons (Student's t-tests), and across time-bins of 1s to fit the behavioural models (regressions). Individual velocities are extracted from the reconstruction of the trajectories, which was based on the identification of each fish from one frame to another (see text).

## 227 **Experimental Validation**

228           Three main experiments were carried out to understand how post-larval convict surgeonfish  
229 (*Acanthurus triostegus*) visually recognize a suitable habitat, adult conspecifics and one of their  
230 predators (bluefin jacks, *Caranx melampygus*). Our first objective was to experimentally validate the  
231 use of simulated 3D models of fishes in a VR setup by confirming that they are realistic enough to  
232 cause natural reactions in post-larval fish.

## 233 **Methods**

### 234 **Specimen collection**

235           Over 200 post-larval *Acanthurus triostegus* (TL = 2.55-2.75 cm) were captured using hand  
236 nets at night, shortly after entering the north-eastern reef crest of Moorea, French Polynesia  
237 (17°29'52.19"S, 149°45'13.55"W). Individual *A. triostegus* had not yet acquired skin stripes which  
238 only form after recruitment, therefore they were still undergoing metamorphosis, and were  
239 considered 'post-larvae' (Besson et al., 2020).

### 240 **Ethical note**

241           Ethical approval for the study was granted from The Animal Ethics Committee, Centre  
242 National de la Recherche Scientifique (permit number 006725). This study also complies with the  
243 rules defined by the Direction de l'Environnement de la Polynésie Française (DIREN) regarding  
244 experiments on coral fish in aquaria. After captured, post-larval fish were placed in acclimatization  
245 aquaria at CRIOBE for 36 hours, in groups of 40 maximum, filled with UV-sterilized and filtered (10-  
246 µm filter) seawater maintained at 28.5 °C, under a 12:12 LD cycle. Stress was minimized during  
247 transport using occluded small aquaria. Once the experiment was over, animals were returned to  
248 their natural habitat.

### 249 **Experimental protocol**

250           The behavioural response to the multiple trials – different habitats or fish shoals – was  
251 assessed for groups of five post-larval fish placed together in the aquarium. A neutral, baseline 3D  
252 environment (sandy bottom with animated caustics) was displayed throughout the experimental  
253 sessions on all five sides of the aquarium. Virtual fish or coral pinnacles appeared and disappeared at  
254 specific times and in specific virtual locations depending on the trial. Each experiment started with a  
255 4 min habituation period in the baseline environment, followed by trials each lasting 90 seconds  
256 (experiment 1 and 2) or 60 seconds (experiment 3). To minimize interference, the baseline  
257 environment was also displayed for 2 min between trials. For each experiment, the presentation  
258 order of trials was randomised and balanced to avoid order effects and allow for statistical  
259 comparisons between pairs of conditions. To exclude possible side biases from the random sand

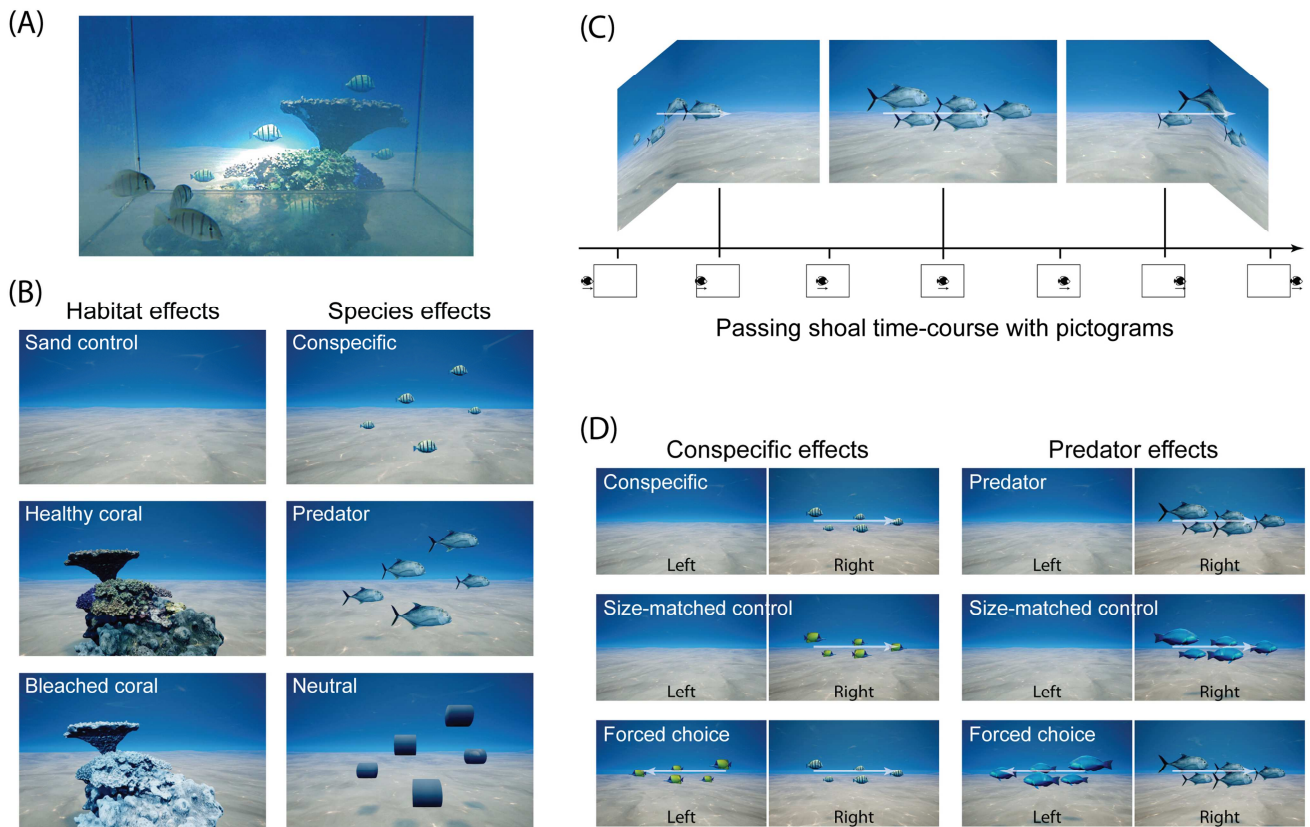
260 texture pattern or from the room's ceiling and lightning, the stimulation side was randomly balanced  
261 between the left and right of the aquarium. Lastly, after every half-day the aquarium was emptied,  
262 washed with freshwater, and refilled and the focal aquarium was oxygenated between replicates.

### 263 **Experiment 1. Effects of static presentation of habitat and fish**

264 Groups of five post-larval fish were presented with six trials: three virtual habitats and three  
265 virtual fish or neutral shapes on only one side of the aquarium (randomised) each for 90 seconds  
266 (**Figure 2B**). Virtual simulations rendered the post-larval fish at a depth of 1.25 m. The three virtual  
267 habitats tested were: Sand control (only the sandy baseline environment); Healthy coral (a pinnacle  
268 with healthy tabular and branched corals); and Bleached coral (the same pinnacle, but all corals were  
269 bleached). The three virtual fish species consisted of shoals of five virtual fish swimming in place in  
270 the same pattern and position: Conspecifics (five adult convict surgeonfish, *Acanthurus triostegus*);  
271 Predators (five bluefin jacks, *Caranx melampygus*); and Neutral (five large untextured cylinders). The  
272 individual positions of five post-larval fish were constantly tracked during the six successive trials  
273 presented in the following order: Sand control (1<sup>st</sup>); Healthy or Bleached coral (randomly 2<sup>nd</sup> or 3<sup>rd</sup>);  
274 Conspecific, Predator or Neutral (randomly 4<sup>th</sup>, 5<sup>th</sup>, or 6<sup>th</sup>). Sixty post-larval fish were tested in 12  
275 groups of 5 fish, and for each the total experimental duration was approximately 22 minutes.

### 276 **Experiment 2. Effects of static versus dynamic presentation of fish**

277 In Experiment 2, with 8 trials, behavioural responses to the static presentation of shoals of  
278 five virtual fish was compared with behavioural responses to a more realistic dynamic situation in  
279 which shoals of five fish appeared, swam past the post-larval fish in a non-aggressive manner and  
280 disappeared. Three virtual fish shoal trials were projected: one static shoal swimming in place (as in  
281 Experiment 1) for 90 seconds; one shoal swimming by during the first 30 seconds, then disappearing,  
282 followed by 60 seconds of the baseline sand environment; or three successive shoals of five fish  
283 swimming nearby and disappearing, each over 30 seconds. In each, virtual shoals swam for 30  
284 seconds at 15 cm/s (slow pace) along a virtual line placed 115 cm from the centre of the test  
285 aquarium, covering a total distance of 4.5 m (**Figure 2C**). The virtual fish shoals were either  
286 surgeonfish conspecifics or bluefin jack predators and were presented in 8 successive trials in the  
287 following order: Sand control (1<sup>st</sup>); Conspecific/Predator static, 1 pass, or 3 passes (randomly  
288 presented in 2<sup>nd</sup>, 3<sup>rd</sup>, or 4<sup>th</sup> position); sand control (5<sup>th</sup>); Conspecific/Predator static, 1 pass, or 3  
289 passes (randomly presented in 6<sup>th</sup>, 7<sup>th</sup>, or 8<sup>th</sup> position). The order in which the fish shoal was  
290 presented (conspecifics or predators first) was varied and the side of the aquarium on which the  
291 virtual fish were presented was randomised. Sixty post-larval fish were tested in 12 groups of 5 post-  
292 larvae, and for each the total experimental duration was approximately 26 minutes.



293  
 294 **Figure 2.** Illustration of the stimuli used in the experiments. **(A)** Rendered scene with virtual corals and  
 295 adult surgeonfish as seen from inside the focal aquarium by real larvae. **(B)** Experiment 1. Habitat  
 296 effects (left): Sand control, Healthy or Bleached coral (pinnacles). Species effects (right): Conspecific  
 297 (adult surgeonfish, *Acanthurus triostegus*), Predator (bluefin jacks, *Caranx melampygus*), Neutral  
 298 (untextured cylinders). The fish stimuli were presented in shoals of five individuals swimming in place,  
 299 centred at a virtual location corresponding to 25 cm behind one of the sides of the test aquarium. **(C)**  
 300 Dynamic presentation of a virtual fish shoal swimming past the post-larval fish (either 1 pass or 3 passes  
 301 for Experiment 2 and only 1 pass for Experiment 3). The virtual fish species were either conspecifics or  
 302 predators (as shown here). Shoals swam along a 4.5-m straight line for 30 seconds at 15 cm/s (slow  
 303 pace). **(D)** Experiment 3. Three conditions were tested to examine the response of the post-larval fish to  
 304 conspecifics (left): Conspecific alone, Conspecific-sized control alone (butterflyfish, *Forcipiger*  
 305 *longirostris*), and Forced choice of conspecific vs. conspecific-sized control. Three conditions were also  
 306 tested to examine the response of the post-larval fish to predators (right): Predator alone, predator-  
 307 sized Control alone (parrotfish, *Scarus psittacus*), and Forced choice of predator vs. predator-sized  
 308 control. Similarly to Experiment 2, the virtual shoals swam along a 6-m straight line for 40 seconds at  
 309 15 cm/s (slow pace).

### 310 **Experiment 3. Effect of size-controlled dynamic presentation of fish**

311 In Experiment 3, behavioural responses to a dynamically swimming shoal of conspecifics or  
 312 predators, was compared with behavioural responses to size-matched heterospecifics. Six virtual fish  
 313 shoal trials were projected (**Figure 2D**): surgeonfish conspecifics on one side; conspecific-sized  
 314 control fish on one side (butterflyfish, *Forcipiger longirostris*); conspecifics and conspecific-sized

315 controls on opposite sides (two-alternative choice); bluefin jack predators on one side; predator-  
316 sized control fish on one side (parrotfish, *Scarus psittacus*); predators and predator-sized controls on  
317 opposite sides (two-alternative choice). Changes in post-larval fish positions from before to after a  
318 virtual shoal swam by were identified. All virtual fish swam at 15 cm/s (slow pace) for 40 seconds  
319 along a virtual line placed at 115 cm from the centre of the aquarium (total distance travelled: 6 m).  
320 The order in which fish shoal types was presented, conspecifics or predators, was balanced between  
321 groups, however, the two-alternative choice was always presented after the single-choice trials. The  
322 order of single-choice trials was also balanced. In all conditions, the stimulus was presented over 40  
323 seconds, and post-larval position recording started 10 seconds before and ended 10 seconds after  
324 the stimulus (total duration of 60 seconds). Eighty post-larval fish were tested in 16 groups of 5 fish,  
325 and for each the total experimental duration was approximately 26 minutes.

### 326 **Data analysis**

327 For all experiments, tracking data was sampled at 5Hz, during 90-second trials for Experiment  
328 1 and 2, and 60-second trials for Experiment 3 (see **Figure 1C**). Representative trajectories of post-  
329 larval groups are available in Appendix **Fig A2**, **Fig A7** and **Fig A11** for Experiment 1, 2 and 3,  
330 respectively. Animated heatmaps of fish position density in the aquarium for all conditions are  
331 available in Appendix **Video A4**, **Video A8** and **Video A12** for Experiment 1, 2 and 3, respectively.  
332 Note that for all 2D plots, data is organized so that the simulation is always presented on the right  
333 side, except for the forced-choice conditions of Experiment 3, for which the stimulation is presented  
334 on both left and right sides. General repeated-measures ANOVAs with trial and 5-second time-bin as  
335 main factors were generated using the four behavioural measures (group centre X- and Y-position,  
336 dispersion and individual velocity). Comparisons between relevant trials (paired Student t-tests) and  
337 the deviation from zero of the group's X and Y positions (Student t-tests against a single value of 0)  
338 were conducted for each time bin. The alpha value for significance was adjusted using Bonferroni's  
339 correction for multiple comparisons on a single dataset and visualized in the plots using different  
340 grey levels (white for  $P > 0.05$  and from light grey for  $P < 0.05/1$  to black for  $P < 0.05/n_{\text{Tests}}$  with  $n_{\text{Tests}} = 3$   
341 for either the 3 paired comparisons or the 3 single-value comparisons). Plots displaying the  
342 timeseries of the four behavioural measures (binned in 5-second intervals) and the results from the  
343 statistical comparisons are provided in the Appendix **Fig A5**, **Fig A9** and **Fig A13** for Experiment 1, 2  
344 and 3, respectively.

### 345 **Behavioural model fit**

346 To characterize the temporal aspect of post-larval fish behavioural responses, we designed  
347 several models taking into account the distance of the post-larval fish to the simulated shoals. The  
348 position of the virtual simulations was sustained and constant throughout the trials in Experiment 1  
349 and in the static trials of Experiment 2, but the virtual shoals moved in the dynamic conditions of

350 Experiments 2 and 3. Because of this major difference between the static and dynamic conditions,  
351 we used a different set of possible behavioural models for either type of trial to measure behaviour  
352 (centre position, individual velocity and dispersion). For the static conditions, we tested three simple  
353 ecologically relevant models (linear, quadratic and exponential) and for dynamic conditions, we  
354 added a periodic component to capture the cyclic variations of the stimulation (**Table 1**). The average  
355 behavioural measures obtained for the tested groups (n=12 or n=16), binned in 1-second intervals,  
356 were fitted using each of the three models. The fit quality was estimated with the root mean square  
357 error (RMSE) between the average data points and the model predictions. In order to avoid data  
358 over-fitting, we used a limited number of models and selected the best model based on the trade-off  
359 between fit quality (RMSE) and the number of parameters. Linear models (for static conditions) and  
360 linear periodic models (for dynamic conditions) have one parameter fewer than the quadratic and  
361 exponential models. They were favoured when the RMSE difference with the other models was  
362 below 5% (e.g., if the linear and quadratic fits had RMSEs of 10 and 9.6 resp., the linear model was  
363 selected). Lastly, in order to check the validity of each fit, the obtained RMSE was compared to the  
364 RMSE distribution obtained by applying, for the given condition and measure, the same fitting  
365 procedure but with scrambled time-bins a thousand times. Two quality criteria were used: if the  
366 obtained RMSE was lower than 0.8 times the mean RMSE distribution, and below the lower 1%  
367 confidence interval bound of the distribution, the fit was considered valid (good signal-to-ratio level).  
368 The results are summarized in plots displaying, for each condition, the time-series of each measure in  
369 bins of 1 second, the best behavioural model fit, and the outcome of the statistical comparisons. For  
370 each condition, the selected model and adjusted parameters are detailed in Appendix **Table A6**,  
371 **Table A10** and **Table A14** for Experiment 1, 2 and 3.

	Name	Equation	Description and meaning of the parameters
Static conditions	Linear	$a \cdot t + b$	Linear models capture responses that change constantly in time. These drifts can be observed in slow responses to a potential danger. $a$ : linear term (drift speed) $b$ : offset (start position)
	Quadratic	$a \cdot t^2 + b \cdot t + c$	Quadratic models capture responses that change constantly in time (1 <sup>st</sup> order) and that have a reversal (2 <sup>nd</sup> order). Reversal are observed of after a loss of interest when attracted by the stimulus ( $a < 0$ if in right side) or after habituation to a fearful stimulus ( $a > 0$ ). $a$ : quadratic term (reversal) $b$ : linear term (drift speed) $c$ : offset (start position)
	Exponential	$l - (l - s) \cdot \exp(-k \cdot t)$	Exponential attenuation models capture natural decaying phenomena within a limited spatial or temporal range. These can be observed in quick escape response to a fearful stimulation. $l$ : limit of the attenuation (reached when $t \rightarrow \infty$ ) $s$ : offset (starting position) $k$ : attenuation factor (positive value, higher for faster decays)
Dynamic conditions	Linear periodic	$a \cdot t + b + \frac{1}{2}A \cdot \cos(2\pi \cdot (t - t_0) / T)$	Linear models combined with a periodic component capture linear drift responses to a cyclic stimulation. Periodic component parameters: $A$ : amplitude of the oscillations (positive value) $t_0$ : phase of the oscillations (peak time, within [0 s, T]) $T$ : period ( <b>fixed parameter</b> set to 30 s and 40 s for Experiment 2 and 3)
	Quadratic periodic	$a \cdot t^2 + b \cdot t + c + \frac{1}{2}A \cdot \cos(2\pi \cdot (t - t_0) / T)$	Quadratic models combined with a periodic component capture 1 <sup>st</sup> and 2 <sup>nd</sup> order responses to a cyclic stimulation.
	Exponential periodic	$l - (l - s) \cdot \exp(-k \cdot t) + \frac{1}{2}A \cdot \cos(2\pi \cdot (t - t_0) / T)$	Exponential attenuation models combined with a periodic component capture naturally decaying periodic responses to a cyclic stimulation.

372

373

374

375

**Table 1.** The sets of behavioural models fitted for the static and dynamic trials. For each model, the equation, the description of the behaviour that it captures, and the meaning of its parameters are detailed.

376

## Results

377

### Experiment 1. Effects of static presentation of habitat and fish

378

379

380

381

382

383

The behavioural responses to the trials were assessed for groups of five post-larval *A. triostegus* placed together in the aquarium. All trials were tested on all groups of post-larval fish. Typical individual trajectories of post-larval fish in response to each of the six trials are shown in Appendix **Fig A2**, scatterplots with all positions occupied by all post-larval fish in Appendix **Fig A3**, and animated heatmaps with the presence density at each successive 1-second intervals in Appendix **Video A4**.

384

#### Habitat effect

385

386

387

388

389

390

Post-larval fish reactions were similar across habitat types (Sand control, Healthy and Bleached coral). Post-larval fish group centre's X- and Y-positions were not significantly different between trials either over the whole test period or for most 5-second intervals (lack of significance in boxes below plots in **Figure 3A** and **B**). Apart from a small positive bias (16.5 px) in the Y-position for the Sand control (entire range:  $t(11)=2.39$ ,  $P < 0.04$ ), possibly related to the initial location in which fish were placed in the aquarium, the X- and Y-positions were not biased to either side of the

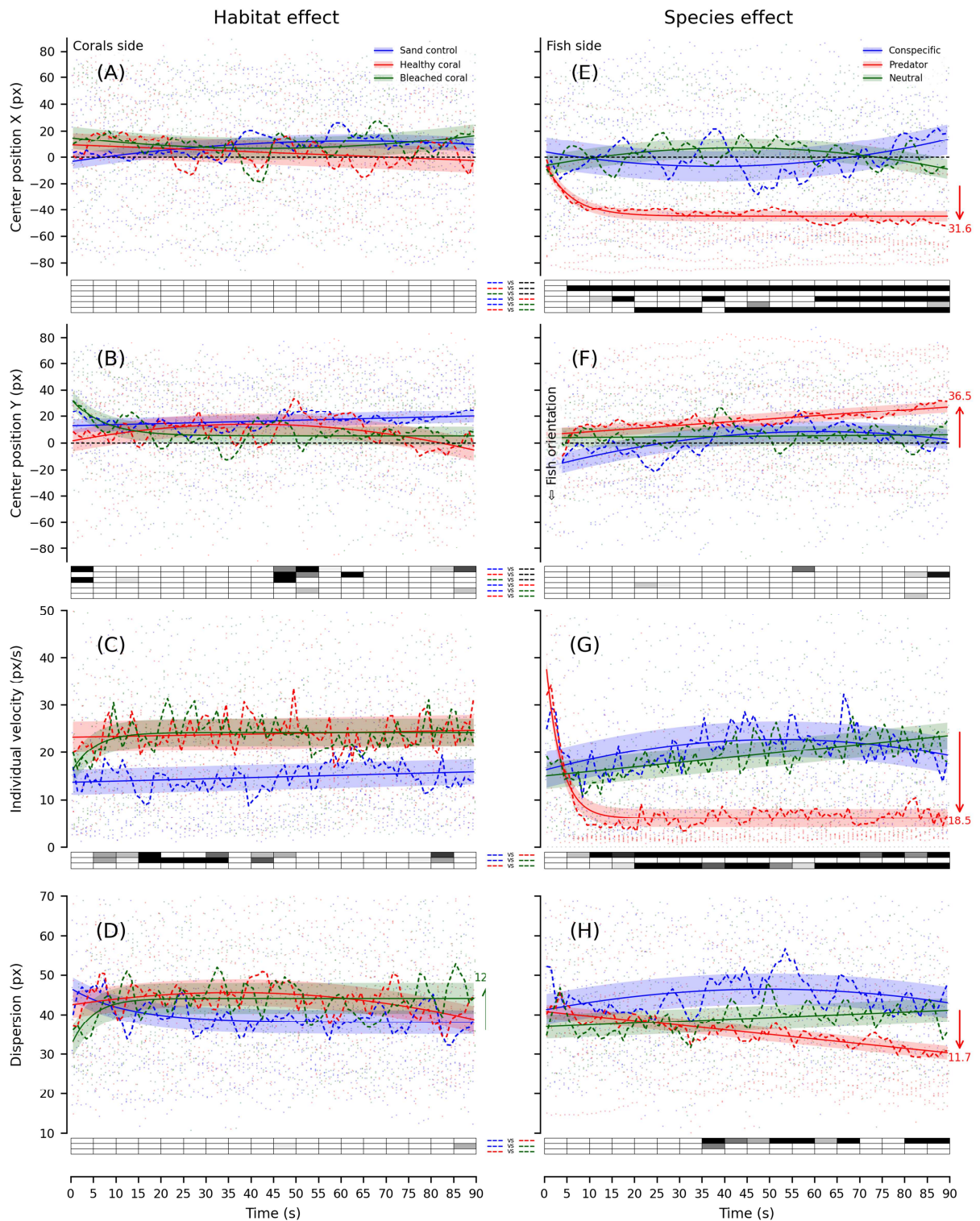
391 aquarium (**Figure 3A and B**). The level of noise did not allow for good quality fits of linear, quadratic  
392 or exponential models (**Table A6**), but the best fit models largely overlapped, confirming non-  
393 significant differences in response behaviours across habitat types. In contrast, there was a  
394 significant effect of habitat on individual velocities ( $F_{2,22}=5.5$ ,  $P<0.015$ ,  $\eta_G^2=0.12$ ), with post-larval fish  
395 moving faster (more activity) when presented with Healthy (23.8 px/s,  $t(11)=2.26$ ,  $P<0.05$ ) and  
396 Bleached (23.7 px/s,  $t(11)=3.11$ ,  $P<0.01$ ) corals compared to no corals in the Sand control (14.7 px/s)  
397 over the whole time range and during some of the 5-second intervals (shaded boxes below plot in  
398 **Figure 3C**). No significant difference in group dispersion – either with statistics or model fitting – was  
399 observed across habitat types (**Figure 3D**).

#### 400 **Species effect**

401 Post-larval fish reactions did not differ when presented with static shoals of conspecifics  
402 (surgeonfish) and neutral cylinders, but were significantly different when presented with predators  
403 (jack fish). Type of fish shoal impacted the post-larval fish group centre's X-position (main effect,  
404  $F_{2,22}=8.3$ ,  $P<0.002$ ,  $\eta_G^2=0.27$ ), which was significantly lower with Predators (–42.3 px) than with  
405 Conspecifics (–1.5 px,  $t(11)=3.14$ ,  $P<0.01$ ) or Neutral cylinders (1.8 px,  $t(11)=3.7$ ,  $P<0.005$ ) across the  
406 entire time-range and for most 5-second intervals (shaded boxes below plot in **Figure 3E**). Post-larval  
407 fish swam away from the virtual predators: they moved 31.6 px from the first to the last time-bin  
408 ( $t(11)=2.83$ ,  $P<0.02$ ), mostly at the beginning of the trial (exponential model with  $k$  parameter of  
409  $0.17\text{ s}^{-1}$ ). On the other hand, with virtual conspecifics post-larval fish hit the sides of the aquarium  
410 near the conspecifics more often compared to neutral cylinders or sand control. There was no global  
411 effect of the type of virtual species on post-larval fish Y-positions across the entire time-range and for  
412 any interval (**Figure 3F**). However, post-larval fish moved slowly toward the upper-left quadrant of  
413 the aquarium – the opposite side to the stimulation – and moved to the back of the virtual shoal  
414 (linear model with a slope of  $a=0.238$  px/s) moving 36.5 px ( $t(11)=3.09$ ,  $P<0.01$ ) behind the virtual  
415 predators, reducing dispersion (Appendix **Video A4**). Type of fish shoal had a significant effect on  
416 individual velocities ( $F(2,22)=11.08$ ,  $P<0.001$ ,  $\eta_G^2=0.20$ ), with lower speeds with Predators (7.3 px/s)  
417 than with Conspecifics (20.9 px/s,  $t(11)=4.09$ ,  $P<0.002$ ) and Neutral cylinders (19.3 px/s,  $t(11)=3.23$ ,  
418  $P<0.01$ ) over the entire time range, and most 5-second intervals (**Figure 3G**). Furthermore, with  
419 predators individual velocities rapidly decreased by 18.5 px/s over the first ten seconds ( $t(11)=3.47$ ,  
420  $P<0.005$ ), remaining at 6.1 px/s until the end of the trial (exponential model with a very high  $k$   
421 parameter value of  $0.30\text{ s}^{-1}$ ). Movement, as well as space occupied in the aquarium, were similar  
422 when presented with surgeonfish, cylinders or only sand (Appendix **Fig A3**). The effect of fish shoal  
423 type on group dispersion was nearly significant ( $F(2,22)=2.89$ ,  $P=0.077$ ,  $\eta_G^2=0.071$ ), due to less  
424 dispersion with Predators (35.5 px) than with Conspecifics (44.9 px) across the entire time range  
425 ( $t(11)=3.37$ ,  $P<0.007$ ), and in most intervals after 35 seconds (**Figure 3H**). With predators, group  
426 dispersion decreased slowly and progressively during the trial (linear model with  $a=-0.12$  px/s), by



427 11.7 px ( $t(11)=2.90$ ,  $P<0.015$ ): post-larval fish tended to gather after detecting a threat. The best-  
428 fitting models of the behavioural reactions to virtual bluefin jacks highlight natural repulsion from a  
429 fear-invoking stimulation: the exponential models captured quick responses in a limited space/time  
430 range (X-position and individual velocity), whereas the linear models captured slow drifting  
431 responses (Y-position and dispersion). In general, the four different behavioural indicators (X and Y  
432 position, individual velocity, and dispersion) were not different between conspecifics and neutral  
433 cylinders, and despite high variability between individuals resulting in poor quality fits, models also  
434 mostly overlapped (**Table A6**). However, when presented with predators, the quality of model fitting  
435 for all behavioural measures was excellent i.e. post-larvae showed homogeneous behaviours within  
436 each group as well as across groups.



437

438

439

440

441

442

443

444

**Figure 3.** Experiment 1 group time series, with best model fits and statistics. X- and Y-positions of the group centre, individual velocity, and group dispersion for Habitat (A-D) and Species trials (E-H). Coloured dashed lines show the average at each time-point of n=12 groups (Habitat trials: Sand control in blue, Healthy coral in red, Bleached coral in green; Species trials: Conspecific in blue, Predator in red, Neutral in green). Coloured lines show the best fitting model for the corresponding trials and error stripes show the RMSE. For each 5-second time-bin, average performances were compared either between each trial or to zero with paired and single-value Student t-tests. Significance levels are

445 provided in the boxes below the plots (ranging from light grey for  $P < 0.05/1$  to black for  $P < 0.05/n_{\text{Tests}}$   
446 using Bonferroni's correction for  $n_{\text{Tests}}=3$ ; white for  $P > 0.05$ ).

## 447 Experiment 2. Effects of static versus dynamic presentation of fish

448 Typical individual trajectories of post-larval *A. triostegus* in response to each of the eight  
449 trials are shown in Appendix **Fig A7**, and animated heatmaps with the presence density at each  
450 successive 1-second interval in Appendix **Video A8**. Sand control trials were presented before the  
451 conspecific and predator trials to provide acclimatization periods. Since no qualitative or statistical  
452 differences in behaviour were observed, these results are not reported here.

### 453 Conspecific effect

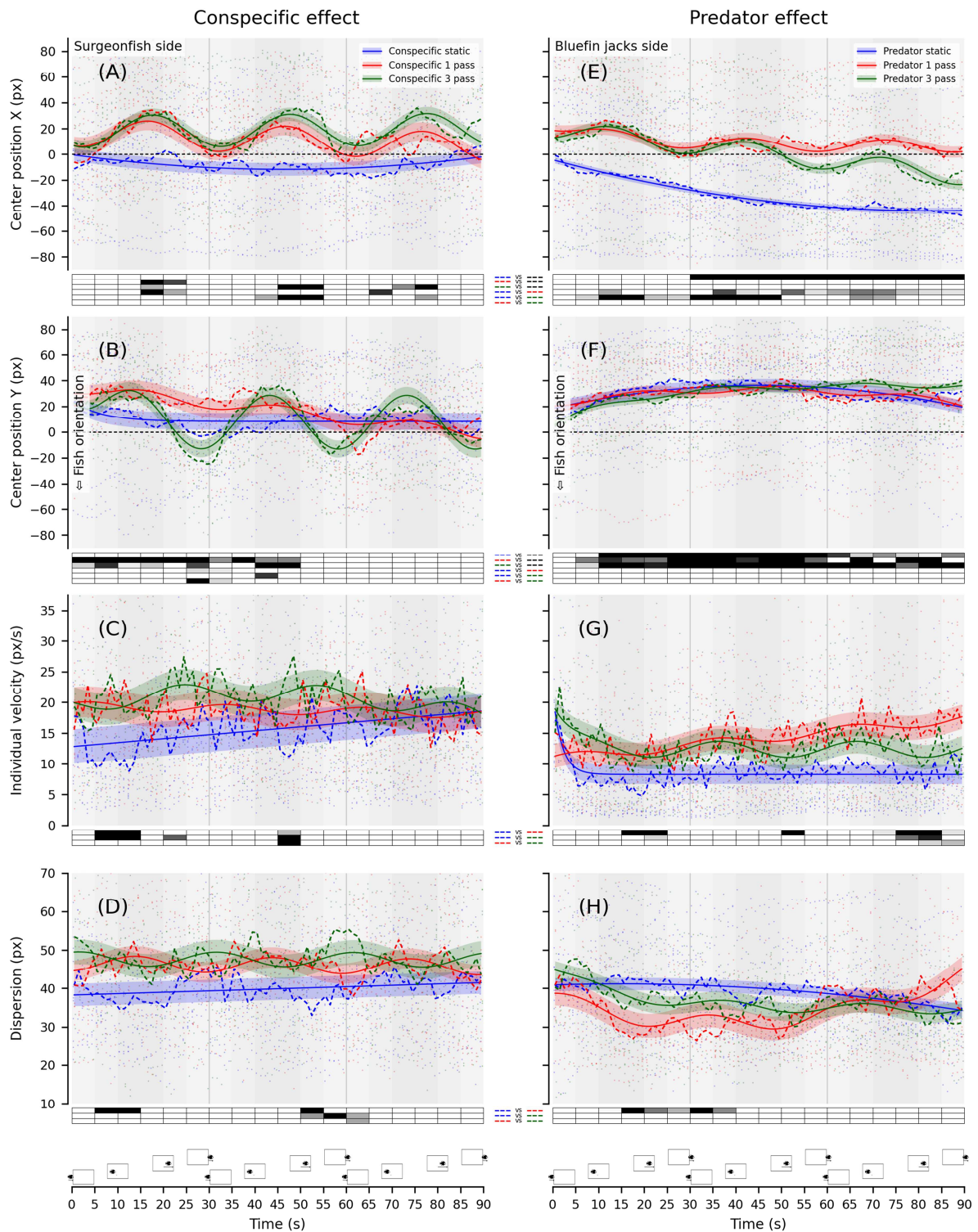
454 Post-larval fish reactions were different when presented with either static (swimming in  
455 place) or dynamic (1- or 3-passes) surgeonfish. In the static trial, groups came close to the  
456 stimulation (hitting the aquarium side), similarly to Experiment 1, and the group centre's X-position  
457 did not deviate significantly from zero. The best-fitting model quadratic only of average fit but its  
458 positive  $a$  parameter suggested an habituation to an initially slightly fear-invoking stimulus (**Figure**  
459 **4A** and **Table A10**). In contrast, in the dynamic 1- or 3-pass trials, post-larval fish joined and moved  
460 with the virtual surgeonfish shoal as it travelled along the aquarium side (oscillating X- and Y-  
461 positions, **Figure 4A** and **B**). When the shoal passed 3 times, post-larval fish kept repeating the same  
462 behaviour periodically, without any noticeable attenuation indicating no loss of interest (**Video A8**).  
463 The linear periodic model was the best fit, as it captured the post-larval fish cyclic response, with a  
464 phase  $t_0$  of approximately 17 s for both 1- and 3-pass tests, and an amplitude  $A$  of 21.6 px (1 pass)  
465 and 24.7 px (3 passes). The linear component had an offset  $b$  of about 14 px for both pass types and  
466 a slope  $a$  of  $-0.13$  px/s (1 pass) and null (3 passes). Oscillations in the X-position showed a significant  
467 deviation from zero toward the stimulation side when the shoal was passing (from 15 to 25 s for both  
468 1- and 3-passes, and from 45 to 55 and 75 to 85 s for 3-passes). For the static trial the group centre's  
469 Y-position did not significantly deviate from zero and the best fit was exponential, but of poor quality  
470 (**Figure 4B**). For the 1-pass trial, the linear periodic model had the best fit, with a similar phase  
471 ( $t_0=15.6$  s) but with a much smaller amplitude ( $A=8.5$  px) than for the X-position. The number of post-  
472 larval fish that followed the single shoal passage (**Video A8**) was too limited to produce a clear  
473 trough, resulting in less vertical motion. Moreover, the linear decay and loss of synchronization in the  
474 model after the first cycle was due to the absence of stimulation after 30 seconds. For the 3-pass  
475 trial, the best fitting model was exponential and periodic, with a strong attenuation factor of  
476  $k=0.177$  s<sup>-1</sup>, rapid oscillations around  $l=7.7$  px, a peak at  $t_0=13.2$  s, and large amplitudes ( $A=41.8$  px)  
477 (**Figure 4B**). The first two oscillations showed significant deviations from zero on peaks and troughs.  
478 The X- and Y-oscillations were synchronized and phase-locked with the three virtual surgeonfish  
479 shoal passes: vertical motion widely overlapped with the shoal's linear displacement along the

480 aquarium side, and the horizontal motion corresponded to the movement of post-larvae closer to  
481 the shoal at each pass. The swimming kinematic analyses of swimming provide evidence of cohesive  
482 group behaviour, in which larvae naturally recognize and follow their conspecifics. Individual  
483 velocities were rapidly significantly lower (at 12 px/s then increased linearly, with a fitted slope of  
484 0.064 px/s) with static compared to dynamic virtual conspecifics (**Figure 4C**). This is consistent with  
485 an initially slightly fearful response. In dynamic trials, individual velocities oscillated around 20 px/s  
486 and decreased to similar values as in static trials towards the end of the trial, but noise was too high  
487 for the periodic models to reach a good fit (**Table A10**). Group dispersion tended to be lower for the  
488 static than dynamic trials, and fit was poor (**Figure 4D**).

### 489 **Predator effect**

490 Post-larval fish reacted very differently in response to static compared to dynamic bluefin  
491 jack shoals. Static presentation produced the same reaction as in Experiment 1: movement to the  
492 opposing side and to the back of the virtual shoal with reduced group dispersion. In the 1- or 3-pass  
493 dynamic tests, the density patterns of heatmaps were bimodal, indicative of two reaction types: one  
494 similar to that of the static trial, while the second was an asynchronized back-and-forth movement in  
495 the X-dimension with the post-larvae moving behind the virtual predators after each pass. The  
496 balance between these two reactions varied, with the proportion of static-like behaviour increasing  
497 through time. In the static condition, the gradual decrease in X-position (significant deviation from  
498 zero in all time-bins beyond 30 seconds) was best fitted with a quadratic model ( $a=0.006 \text{ px/s}^2$ ,  $b=-$   
499  $0.96 \text{ px/s}$  and  $c=-4.3 \text{ px}$ ), with parameters for the climax and reversal outside of the trial time-range  
500 (**Figure 4E** and **Table A10**). The best fitting model for the 3-pass condition was linear periodic, with  
501 peaks occurring earlier than with conspecifics ( $t_0=12.8 \text{ s}$ ), a limited amplitude ( $A=14.6 \text{ px}$ ), and a  
502 linear drift (slope  $a=-0.404$ ) of post-larval fish that gradually moved to the opposing aquarium side.  
503 For the 1-pass trial, the response to the first pass overlapped with that of the 3-pass ( $t_0=12.7 \text{ s}$  and  
504  $A=9.5 \text{ px}$ ) and after this pass, oscillations and drifting were exponentially attenuated. None of the X-  
505 positions in the dynamic scenario deviated significantly from zero, but post-larval fish were  
506 significantly closer to the stimulation side than in the static trial over multiple time bins. The Y-  
507 position was very similar in the three trials (**Figure 4F**): post-larvae moved rapidly behind bluefin jack  
508 shoals whether swimming in place (quadratic model) or passing nearby once (quadratic periodic) or  
509 three times (exponential periodic). Despite good quality fits, these models largely overlapped and  
510 deviated significantly from the midline zero in almost every time bin after the first 5 seconds. At the  
511 end of the trials, post-larvae tended to move back towards the midline in the static condition  
512 (habituation) and in the 1-pass condition (no more stimulation). Consistent with Experiment 1,  
513 individual velocity in the static trial decreased rapidly from 21.3 px/s ( $k=0.50 \text{ s}^{-1}$ ) to 8.2 px/s, which  
514 matched an exponential attenuation model (**Figure 4G**). In the 3-pass condition, post-larval velocities  
515 fit an exponential periodic model, decreasing rapidly from 19.4 px/s ( $k=0.27 \text{ s}^{-1}$ ) to oscillate around

516 12.4 px/s at small amplitude ( $A=2.6$  px). Furthermore, velocities decreased when post-larval fish  
517 noticed predators at each new pass (peak phases locked to  $t_0=6.5$  s). In the 1-pass trial, oscillations  
518 had a lower amplitude ( $A=1.5$  px), and individual velocities increased linearly after the shoal pass,  
519 with underlying oscillations starting once speeds exceeded 10.9 px/s. The only difference between  
520 trials occurred towards the end of the static and 1-pass trials, when post-larval fish swam faster in  
521 the absence of stimulation. Group dispersion was lower for the dynamic 1-pass than for static trials  
522 (15-40 seconds; **Figure 4H**), increasing again in the absence of stimulation (quadratic periodic model).  
523 In the static trial, dispersion decreased slowly (quadratic model) but less than in Experiment 1,  
524 possibly due to the influence of dynamic trials used in the design. In the 3-pass trial, dispersion was  
525 exponentially attenuated, starting at 45 px dropping almost linearly to 34 px (low  $k$  factor of  $0.06$  s<sup>-1</sup>).



526

527

528

529

530

531

532

533

534

**Figure 4.** Experiment 2 group time series, with best model fits and statistics. X- and Y-positions of the group centre, individual velocity, and group dispersion for Conspecific (A-D) and Predator trials (E-H). Coloured dashed-lines show the average at each time-point of n=12 groups (Conspecifics and Predator trials: static in blue, 1 pass in red, 3 pass in green). Coloured lines show the best fitting model for the corresponding trials and error stripes show the RMSE. For each 5-second time-bin, average performances were compared either between each trial or to zero with paired and single-value Student t-tests. Significance level is provided in the boxes below the plots (ranging from light grey for  $P < 0.05/1$  to black for  $P < 0.05/n_{\text{Tests}}$  using Bonferroni's correction for  $n_{\text{Tests}}=3$ ; white for  $P > 0.05$ ). Shaded areas

535 highlight the stimuli critical periods based on the on-going distance of the virtual shoals in the 3-pass  
536 conditions (30-second periodicity) illustrated by the fish positions relative to the side screen shown  
537 above the time axis.

### 538 **Experiment 3. Effect of size-controlled dynamic presentation of fish**

539 Typical individual trajectories of post-larval *A. triostegus* in response to each of the six trials  
540 are shown in Appendix **Fig A11**, and animated heatmaps with the presence density at each  
541 successive 1-second interval in Appendix **Video A12**. Contrary to previous experiments, model fitting  
542 was limited to the interval of 10-50 s, during which the stimulus was visible: the cycle duration of the  
543 periodic component was set to 40 s.

#### 544 **Conspecific effect**

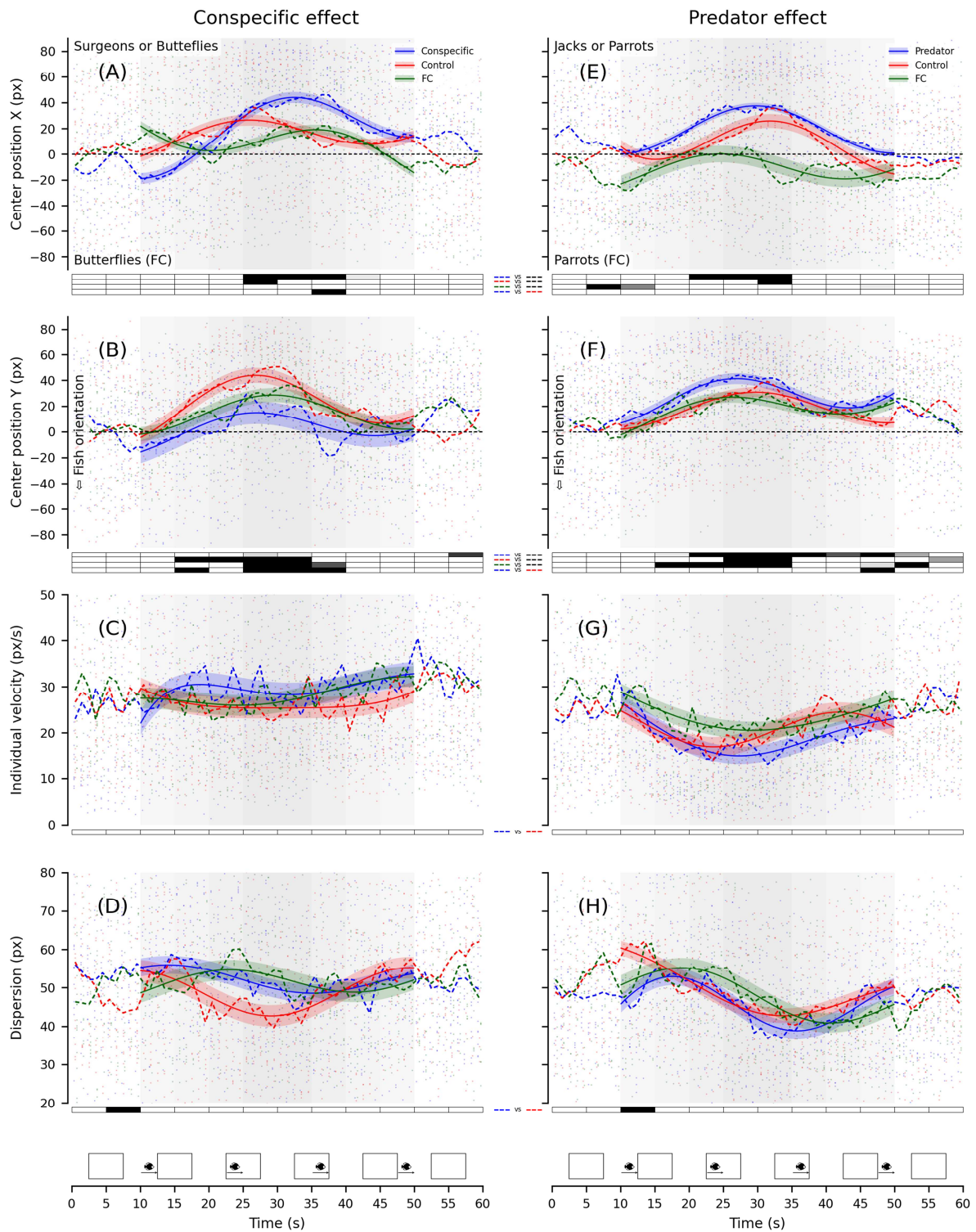
545 Post-larval fish reactions to virtual conspecific surgeonfish or control size-matched  
546 butterflyfish passing nearby were mostly similar, yet with subtle differences. Post-larval fish showed  
547 the same behaviour as in Experiment 2: they moved to the upper-right quadrant, but fewer post-  
548 larval fish followed the virtual shoal of non-aggressive size-matched controls along the Y-axis  
549 compared to conspecifics. Furthermore, dispersion increased faster in the Control compared to  
550 Conspecific trials. When both conspecifics and controls were presented (Forced choice), most post-  
551 larval fish gathered on the conspecifics side and followed the shoal. The best model for all conditions  
552 was linear periodic, except when stated otherwise (**Table A14**). The linear components of the change  
553 in X-positions in the Conspecific and Control trials were positive, suggesting an increase in interest  
554 over the trial (**Figure 5A**). However, the oscillation during the single pass had a larger amplitude and  
555 peaked a few seconds later for surgeonfish ( $A=45.7$  px and  $t_0=31$  s) than control butterflyfish  
556 ( $A=26.3$  px and  $t_0=24$  s). The time interval during which the X-position deviated significantly from the  
557 midline was wider for conspecifics (more than three time-bins compared to a single one) and there  
558 was a significant difference in X-position between the Control and Conspecific trials during the 35-  
559 40 s interval. The linear component of the Y-position in both the Conspecific and Control trials had  
560 the same positive slope ( $a\approx 0.4$  px/s) and oscillation phase ( $t_0\approx 26$  s), but the amplitude in the  
561 Conspecific trial was smaller ( $A=26$  px against 46 px, **Figure 5B**). The Y-position did not deviate from  
562 the midline, and was significantly higher in the Control trial. When both fish shoals were presented  
563 (Forced choice), post-larval fish responses were less intense than when presented with only one  
564 stimulation but still showed the same two reaction types, *i.e.*, following the conspecifics or remaining  
565 in the upper-left quadrant. The X-position was positive and peaked at  $t_0=38$  s, but deviation from  
566 midline was not significant due to a strong linear decrease ( $a=-0.92$ ). Altogether, these results  
567 indicate that post-larval fish were more attracted to and followed conspecific surgeonfish, whilst  
568 spending more time in the upper-right quadrant with similarly-sized butterflyfish. Individual velocity  
569 measurements were noisy but remained relatively constant throughout the three trials (at 30 px/s),

570 with fits that mostly overlapped (**Figure 5C**). The linear component of the good quality fit group  
571 dispersion model was similar in all three trials, with a nearly null slope (constant) at  $b \approx 50$  px (**Figure**  
572 **5D**). There were differences in the periodic component, with oscillations of smaller amplitude and  
573 troughing 6s later with Conspecifics ( $A=6.6$ ) compared to Controls ( $A=12.2$  px), confirming that  
574 dispersion increased faster after the butterflyfish shoal passed than after the conspecifics.

### 575 **Predator effect**

576 Heatmaps of post-larval fish position density highlight subtle differences in their reaction to  
577 dynamic virtual predators versus control parrotfish. With predators, post-larval fish rapidly moved to  
578 the upper-right quadrant and remained at the back of the shoal. In contrast, with non-aggressive  
579 size-matched controls, post-larval fish also gathered in the upper-right quadrant, but some rapidly  
580 started to follow the shoal: group dispersion increased more and earlier than with predators. When  
581 both predators and non-aggressive controls were presented (Forced choice), most post-larval fish  
582 gathered in the upper-left quadrant with controls, with only a few staying on the predator side or  
583 following either predators or controls. The periodic component of the X-position for the Predator  
584 trial was smaller and peaked earlier ( $A=36.9$  px and  $t_0=29.7$  s) than for Controls ( $A=41.6$  px and  
585  $t_0=32$  s, **Table A14**): with bluefin jacks, post-larval fish moved more to the stimulation side and earlier  
586 (20-35 s) than with parrotfish (30-35 s, **Figure 5E**). When both fish shoals were presented (Forced  
587 choice), X-position of post-larval fish fluctuated around the midline ( $b=-19.4$  px and  $A=25.1$  px), with  
588 a non-significant deviation towards parrotfish. The periodic component of the Y-position peaked for  
589 all conditions at similar times ( $t_0=24.2-29.6$  s), with post-larval fish moving rapidly behind fish shoals  
590 (**Figure 5F**), especially with predators. However, the combined periodic amplitude and quadratic  
591 component in the predator trial, and the linear component in the forced choice task, indicated that,  
592 while post-larval fish tended to follow parrotfish and were distributed centrally along the Y-axis at  
593 the end of the stimulation (deviating from midline only in the 25-35 s interval), they remained in the  
594 upper-half of the aquarium behind virtual predators (Y-position always positive throughout the  
595 stimulation). Across the three trials, individual velocities decreased rapidly to about 20 px/s, with  
596 troughs at similar times ( $t_0=22.8-25.8$  s). However, model fit of velocity had a quadratic component  
597 highlighting that velocity decreased over a longer period of time in the Predator compared to Control  
598 trial before increasing again (**Figure 5G; Table A14**). Dispersion decreased earlier than velocities and  
599 increased slower with Predators (trough at 35.5 s) than Controls (trough at 31.9 s) although not  
600 statistically significant (**Figure 5H**).





601

602

603

604

605

606

607

608

609

**Figure 5.** Experiment 3 group time series, with best model fits and statistics. X- and Y-positions of the group centre, individual velocity, and group dispersion for Conspecific (**A-D**) and Predator trials (**E-H**). Coloured dashed-lines show the average at each time-point of  $n=16$  groups (Conspecific trials: Conspecific in blue, Control in red, Forced-choice in green; Predator trials: Predator in blue, Coloured lines show the best fitting model for the corresponding trials and error stripes show the RMSE. For each 5-second time-bin, average performances were compared either between each trial or to zero with paired and single-value Student t-tests. Significance level is provided in the boxes below the plots (ranging from light grey for  $P<0.05/1$  to black for  $P<0.05/n_{\text{Tests}}$  using Bonferroni's correction for  $n_{\text{Tests}}=3$ ;

610 white for  $P > 0.05$ ). Shaded areas highlight the stimuli critical period based on the on-going distance of  
611 the passing virtual shoals illustrated by the fish positions relative to the side screen shown above the  
612 time axis.

## 613 Discussion

614 Virtual corals – healthy or bleached – displayed on one aquarium side had a significant effect  
615 on post-larval fish behaviour (**Figure 3A-D**). Post-larval fish swimming speed increased and the time  
616 spent close to the aquarium side displaying the simulated corals increased compared to sand  
617 controls with no corals. Interestingly, both healthy and bleached corals attracted post-larval fish. As  
618 herbivores, corals are not part of the diet of *A. triostegus*, so this attraction may be due to  
619 anfractuositities in the coral framework, potentially providing shelter and/or a hiding place (Leis &  
620 McCormick, 2002). In addition, displays of virtual fish highlighted clear and distinct behavioural  
621 responses in post-larval *A. triostegus* (**Figure 3E-H**). When presented with five virtual 3D adult  
622 conspecifics, post-larval fish were attracted to them within ten to twenty seconds. In contrast, when  
623 presented with their natural predators, five virtual bluefin jacks (*C. melampygus*) (Siu et al., 2017),  
624 post-larval fish moved to the opposite side of the aquarium with a rapidly decreasing velocity, and  
625 then slowly gathered behind the virtual predator shoal. These contrasting responses highlight the  
626 ability of these post-larval coral reef fish to visually identify virtual conspecifics and predators and  
627 respond differently, with either attraction (conspecifics) or repulsion and/or avoidance (predators),  
628 consistent with expectations from natural behaviours. Furthermore, the movement of post-larval fish  
629 behind the predator shoal not only confirms their recognition of the virtual predator but also of  
630 virtual body features (distinguishing head from tail and positioning themselves accordingly).

631 The presentation of static or dynamically moving conspecifics led to contrasted reactions in  
632 post-larval fish (**Figure 4A-D**). The sudden appearance of a static conspecific shoal startled post-larval  
633 fish, causing them to move away or remain stationary, but then they showed attraction, even hitting  
634 the side of the aquarium where conspecifics were displayed. However, when the virtual conspecific  
635 shoals appeared 2.5 meters away and slowly got closer, no startle responses were observed, rather  
636 post-larval fish followed the virtual shoals along the side of the aquarium, even after three identical  
637 passes. This dynamic scenario is particularly interesting as it highlights the post-larval fish's natural  
638 cohesive group behaviour, even with virtual conspecifics. Such shoaling and cohesive behaviours  
639 with virtual conspecifics have previously been observed in other experiments (e.g., in adult zebrafish  
640 *Danio rerio*, Saverino & Gerlai, 2008). In contrast, when static predators suddenly appeared on one  
641 aquarium side, post-larval fish slowly moved to the opposite side of the aquarium and gathered  
642 behind the virtual predator shoal (**Figure 4E-H**). When virtual bluefin jacks swam by, the reaction of  
643 the post-larval fish was less clear across individuals, but mostly consisted of an overall decrease in  
644 swimming speed and/or synchronized movements to hide behind the moving virtual predators.

645 When virtual bluefin jacks passed three times, the static-like behaviour became more frequent and  
646 individual swimming speeds decreased with each new pass.

647 We then tested whether these post-larval fish responses were simply due to the size of  
648 virtual fish – repulsion to larger fish and attraction to smaller fish – or whether post-larval fish are  
649 able to differentiate between virtual fish species. We found subtle yet noticeable differences in post-  
650 larval fish reactions to virtual shoals of same-sized non-aggressive controls, butterflyfish *Forcipiger*  
651 *longirostris* and parrotfish *Scarus psittacus*, compared to conspecifics (surgeonfish) and predators  
652 (bluefin jacks) respectively. Post-larval fish showed stronger and longer-lasting attraction towards  
653 conspecifics with clear shoal-following behaviour and less dispersion, compared to butterflyfish and a  
654 preference for conspecifics when both were presented simultaneously (forced choice, **Figure 5A-D**).  
655 When presented with predators, the post-larval fish's back-and-forth escape reaction was triggered  
656 earlier, post-larval fish gathered behind the virtual fish for longer and displayed periods with reduced  
657 velocity and dispersion at each shoal passage compared to parrotfish (**Figure 5E-H**). In the forced  
658 choice task, post-larval fish had a tendency to prefer size-matched parrotfish rather than predators.  
659 Altogether, these findings provide evidence that, based on visual cues alone, post-larval fish can  
660 distinguish a conspecific from an equally small but non-aggressive fish species, and a predator from  
661 an equally large but non-aggressive fish species, suggesting that post-larval surgeonfish respond  
662 behaviourally not only to size, but also to the shape and colour pattern of virtual fish.

663 Over the last two decades, a range of studies have demonstrated that post-larval fish possess  
664 developed behavioural and sensory abilities, rejecting the traditional paradigm that they are passive  
665 plankton (Leis, 2015; Beldade et al., 2012, 2016). In particular, post-larval fish survival depends on  
666 their ability to correctly evaluate sensory cues and select appropriate behavioural responses, *e.g.*,  
667 move toward conspecifics or flee predators (Barth et al., 2015). Among the sensory cues used by  
668 coral reef post-larval fish, visual cues are the most discussed, but their importance is the least  
669 understood (Lecchini et al., 2014). The visual abilities of post-larval fish increase during their pelagic  
670 life to reach a maximum near the onset of metamorphosis (Lara, 2001). Our experiments yield  
671 convincing and quantified behavioural results highlighting the role of visual cues in post-larval fishes  
672 at a stage in their development during which they seek a suitable recruitment habitat. In particular,  
673 post-larval *A. triostegus* showed marked attraction towards corals, potentially due to the complex 3D  
674 structures with which they are associated. Furthermore, post-larval fish used visual cues to  
675 discriminate between conspecifics and predators and tailor their movement and behaviour to either  
676 follow their conspecifics (in ecological settings, this could be used to find a suitable settlement  
677 habitat) or avoid predation.

## 678 VR for Behavioural Studies

### 679 Proof of concept

680 The experimental program shows that coral reef post-larval convict surgeonfish (*Acanthurus*  
681 *triostegus*) visually recognize possible hiding places, adult conspecifics, and bluefin jack (*Caranx*  
682 *melampygus*) predators, presented virtually. These results provide a successful proof of concept of  
683 our innovative virtual reality setup with automated tracking of fish responses to simulated 3D models  
684 of habitats and fish shoals. We overcame two technical challenges: we simulated 3D models of fishes  
685 and habitats that were realistic enough to elicit natural reactions in post-larval coral reef fish, and we  
686 detected their individual positions in the aquarium in real-time during the trials using a video-based  
687 tracking system. The detailed behavioural reactions of *A. triostegus* post-larvae to conspecifics and  
688 predators through several relevant kinematic measures such as their position in the aquarium,  
689 individual swimming speed, and group dispersion and the multi-factorial analysis of these measures  
690 enabled us to disentangle responses that could yield very similar results in less controlled  
691 experimental designs (sand vs. corals, parrotfish vs. bluefin jacks, butterflyfish vs. surgeonfish).

### 692 Current limitations and solutions

693 In this project, we relied on the Microsoft Kinect Azure depth camera, an IR-based  
694 technology that proved unsuitable for underwater tracking, forcing us to only use its embedded  
695 colour camera. Tracking with a single camera limits the detection of fish in the aquarium to 2D  
696 horizontal positions, so we blocked the real-time updating of the viewpoint (see Video-based  
697 tracking section). Rendering of the animated scene was however geometrically correct at the centre,  
698 and distortions remained limited within the focal aquaria. We believe the behavioural response to  
699 the presentation of virtual coral reef habitats would be stronger with the real-time updating of the  
700 viewpoint, by enhancing the fish sensation of physically reaching the virtual anfractuositities. To  
701 overcome these limitations in our future projects, we recently updated the VR setup to include a pair  
702 of high-resolution colour cameras, and developed a complex underwater calibration procedure.  
703 Today we can triangulate the detected fish positions from each view, in order to compute in real-  
704 time a fish's 3D position and update the rendering viewpoint in the virtual scene accordingly.  
705 Coupling tracking data with the simulation also allows placing the desired test stimulus in the line of  
706 sight of focal individuals.

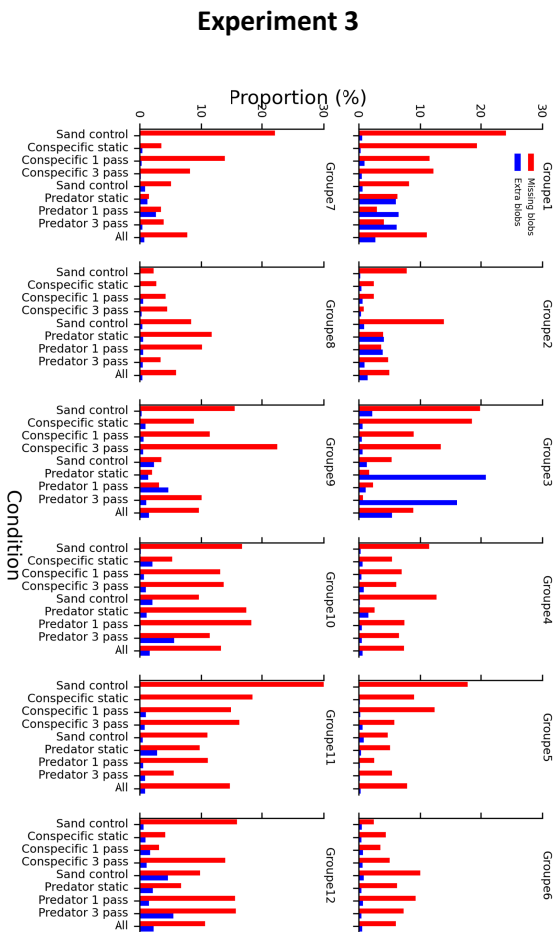
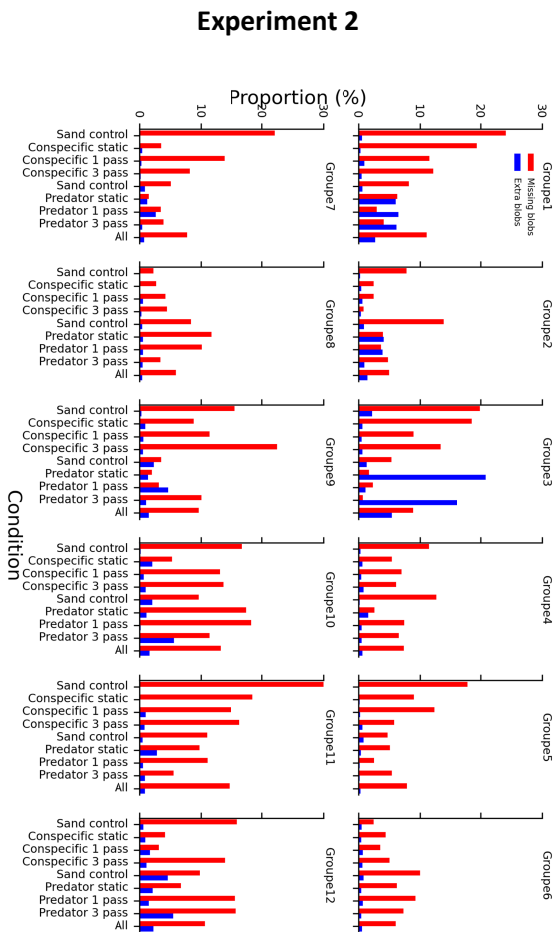
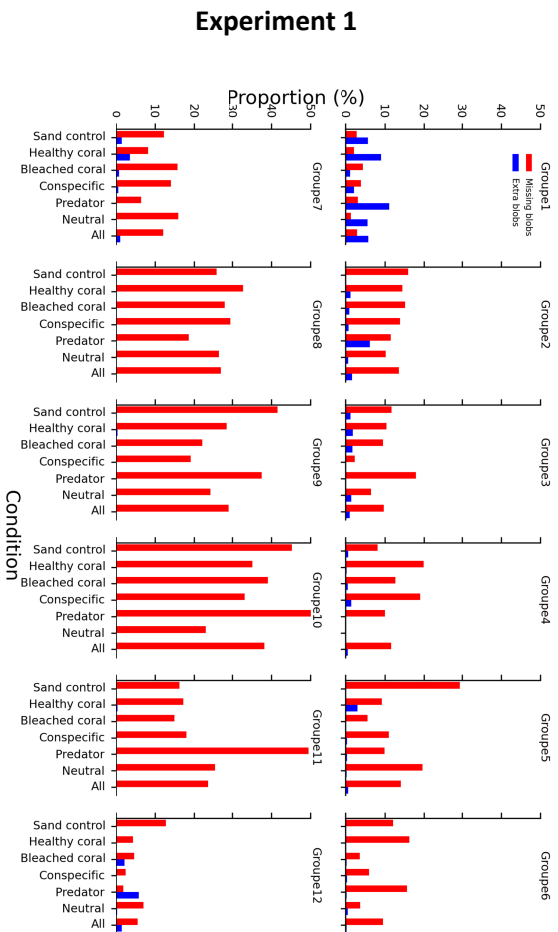
### 707 Perspectives

708 Numerous other simulations could be used with such experimental setup to test a wide  
709 variety of parameters on coral reef fishes at different stages of development, or test coral reef fishes

710 reared in different conditions or exposed to different stresses prior to the visual cue experiment, and  
711 quantitatively characterize the impact on their behaviour. The use of VR offers countless new  
712 research opportunities including to better understand behaviours of coral reef fish in response to  
713 local and global changes (Beldade et al., 2017; Mills et al., 2020; Nedelec et al., 2017; Schligler et al.,  
714 2021) and how they impact the role of vision in habitat selection at recruitment. To understand the  
715 mechanisms involved in the visual recognition of conspecifics or predators, our VR set-up can be  
716 used to manipulate as many visual factors as needed, including size, colour patterns, fin  
717 arrangements, but also the behaviour of other individuals (aggressive, curious, social, fleeing). Even if  
718 some experimental protocols in aquaria partially control for these factors and facilitate observations  
719 compared to *in situ* protocols (e.g. Katzir, 1981; Roux et al., 2016; Besson et al., 2017), the  
720 acclimation time required to perform experiments limits the range of possible manipulations. In  
721 addition, when real fish are used as stimuli (e.g. Lecchini et al., 2014), the experiment cannot be  
722 reproduced multiple times in a reliably comparable manner, as the movement of the stimulus fish  
723 cannot be controlled. This study demonstrates that VR, even with a static rendering viewpoint,  
724 provides an excellent methodology to apply perfectly-controlled virtual stimuli, which post-larval fish  
725 are able to correctly identify. VR can reproduce fairly realistic natural situations that can yield robust  
726 statistical results and allow for highly-precise quantifications of post-larval behaviour in response to  
727 highly diverse scenarios. In addition, video-based modern tracking technologies have recently  
728 emerged in the field of animal behaviour and neuroscience, offering the possibility to conduct fine-  
729 grained kinematic analyses of the reactions of animals to specific situations (Portugues & Engert,  
730 2009; Harvey et al., 2009; Barker & Baier, 2015; Dunn et al., 2016; Stowers et al., 2017; Larsch &  
731 Baier, 2018; Drew, 2019; Harpaz et al., 2021).

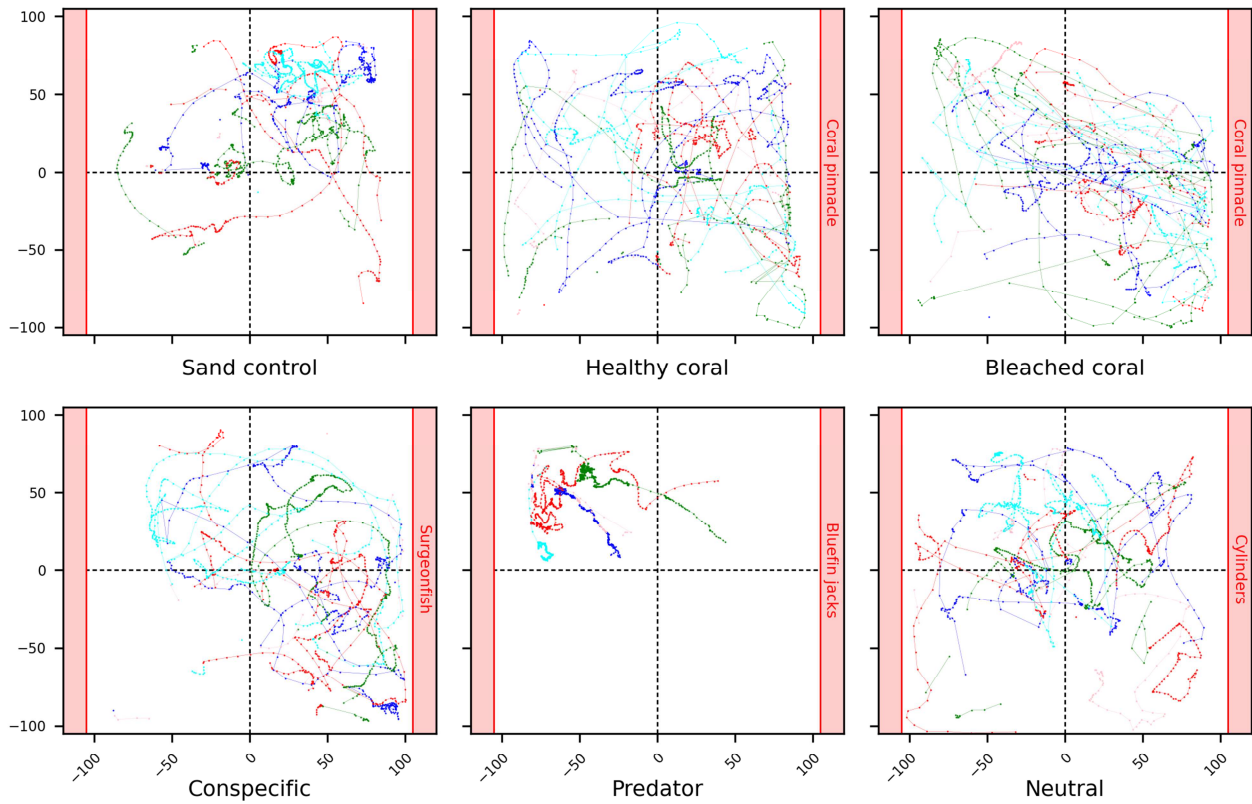
732 In conclusion, we show proof of concept of our new VR visual stimulation set-up combined  
733 with an automated tracking system in an aquarium. The benefits and disadvantages of studying fish  
734 behaviour with such technology are listed here. Benefits include shorter habituation phases in the  
735 aquarium (approximately 30 seconds, compared to 5-7 minutes when experimenting with non-VR  
736 methods, see Nanninga et al., 2017), which we attributed to the non-aggressive immersive baseline  
737 environment; a perfect control of visual stimulation (timing and content) allowing for the same  
738 stimulations to be repeated within or between individuals several times; the possibility to test the  
739 same individuals in multiple successive trials, and in a controlled order; and, as mentioned earlier,  
740 the setup enabled us to automatically collect numerous parameters about the kinematics of fish  
741 reactions in real-time, which contributed to a precise and objective characterization of their  
742 behaviour. Disadvantages include testing the behaviour of fish in a laboratory setting out of their  
743 natural milieu, with a visual rendering that cannot reach the quality of a real environment; and the  
744 technical skills in computer science required to prepare experiments and to process the large  
745 amount of data. However, this successful proof of concept of our new VR setup and automated

746 tracking system on relatively fragile and small post-larval coral reef fish in response to both habitats  
747 and different fish species holds significant promise for the field of fish behavioural ecology across all  
748 life-stages and fish species in response to multiple biotic and abiotic conditions. The experimental  
749 set-up can be scaled up or down as a function of the size of the focal fish and, as such, our VR set-up  
750 holds tremendous promise for the future of the study of teleost behaviour.



753 **Fig A1.** Tracking performance for each experiment and tested fish group in all conditions. The average  
754 proportions of missing/extra blobs are given in red/blue. Tracking accuracy was evaluated by computing  
755 the average proportion of detected blobs relative to the number of expected blobs (5 per frame) across  
756 all recorded frames of the trial. In Experiment 1, on average, 16.3% blobs were missing, and 1.0% extra  
757 blobs were detected. The tracking was rather poor for 4 groups (8, 9, 10 and 11), for which there were  
758 on average 29.3% missing blobs. However, these groups remained in the analyses as the sampling rate  
759 of 5Hz was high enough for the overall data to be valid. In order to improve the tracking performance,  
760 we reduced the luminosity variations by using opaque black curtains for the experimental room's  
761 windows. In Experiment 2 and 3, 8.9% and 10.9% of blobs were missing, and 1.5% and 1.3% extra blobs  
762 were detected on average respectively.





763

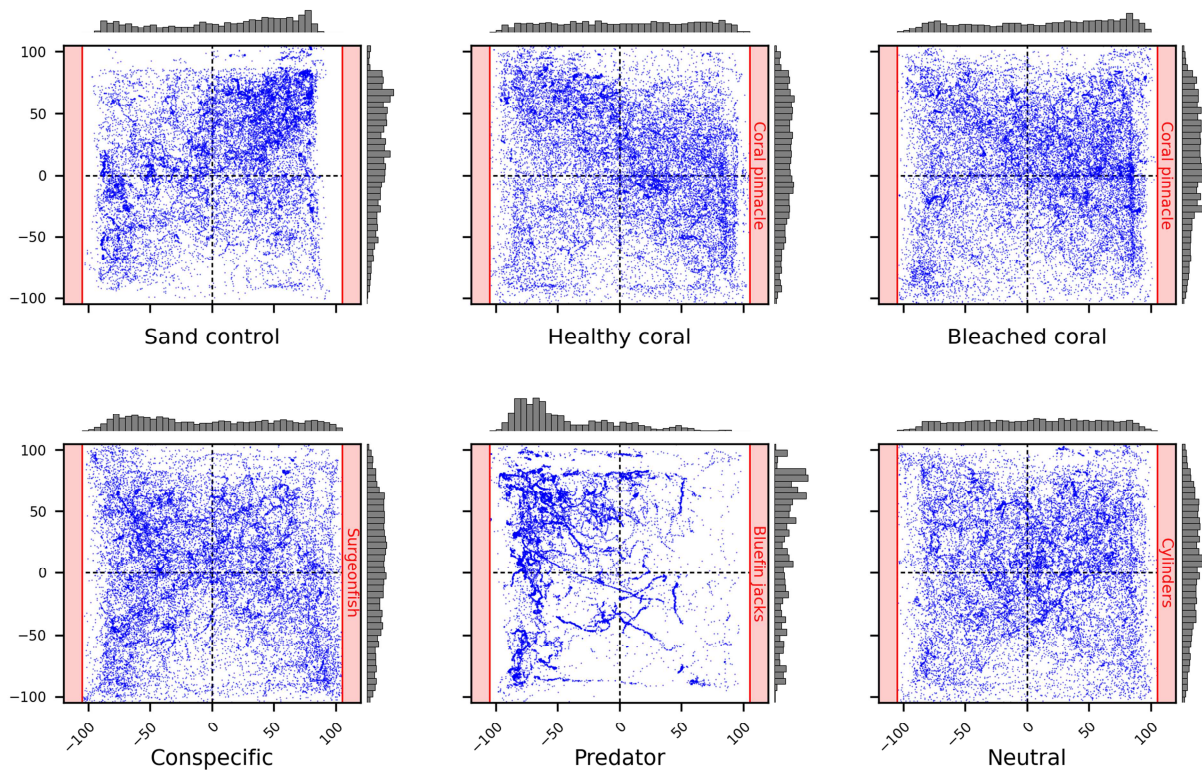
764

765

766

767

**Fig A2.** Example of individual trajectories reconstruction in Experiment 1. Individual fish trajectories illustrating behavioural reactions of a typical group to the 6 stimuli presented on the aquarium sides (red shaded areas) of Experiment 1. The validated positions of fish are connected by coloured lines using a minimal distance heuristic to track individual fish in successive frames.



768

769

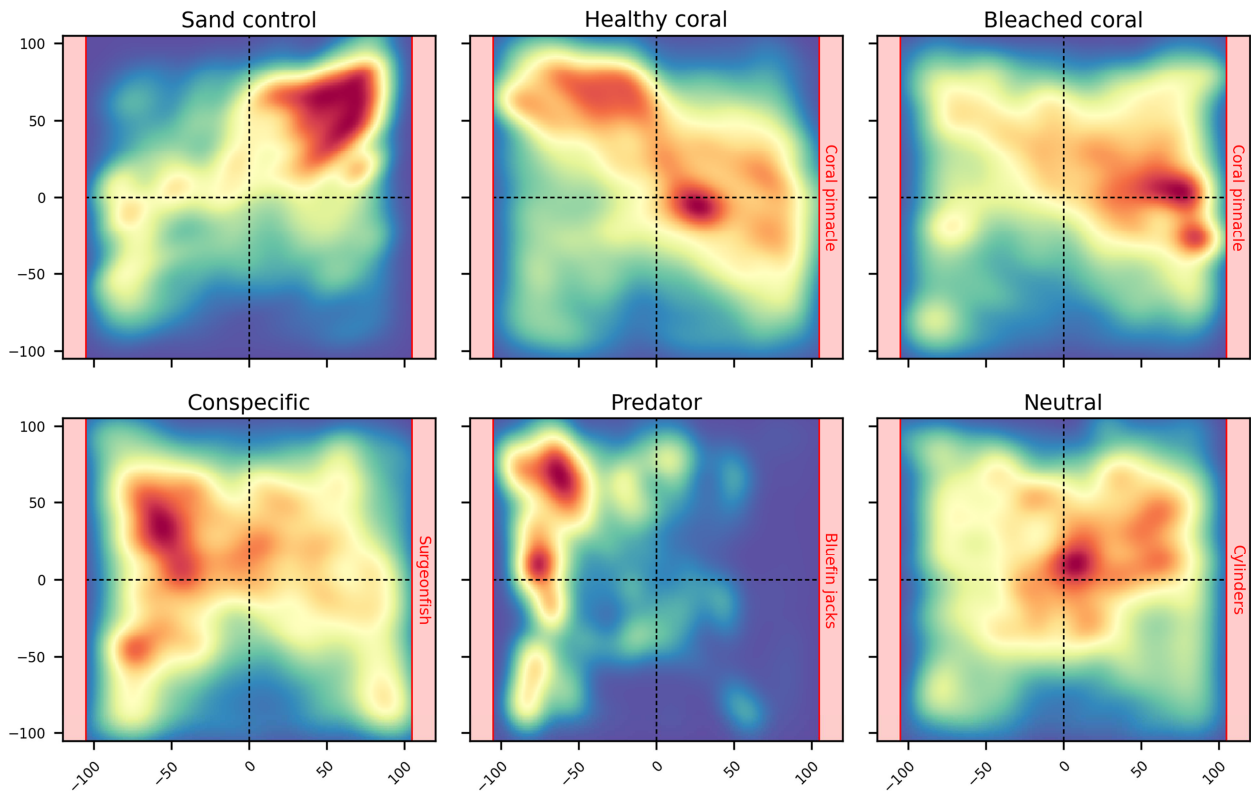
770

771

772

773

**Fig A3.** Experiment 1 raw results visualization. 2D positions of all fish and all groups (n=12), in the 6 tested conditions: Sand control, Healthy coral, Bleached coral, Conspecific, Predator, and Neutral. For each condition, the stimulation was presented on the right side. All valid positions detected at each frame throughout trial durations are presented. Normalized X- and Y-position distribution histograms are provided above and to the right of each plot.



774

775

**Video A4.** Animation showing the average behavioural responses of Experiment 1. Heatmaps for each  
 776 condition where fish position density in the aquarium is plotted in successive intervals of 1 second.  
 777 Density ranges from low (dark blue) to high (dark red).

778

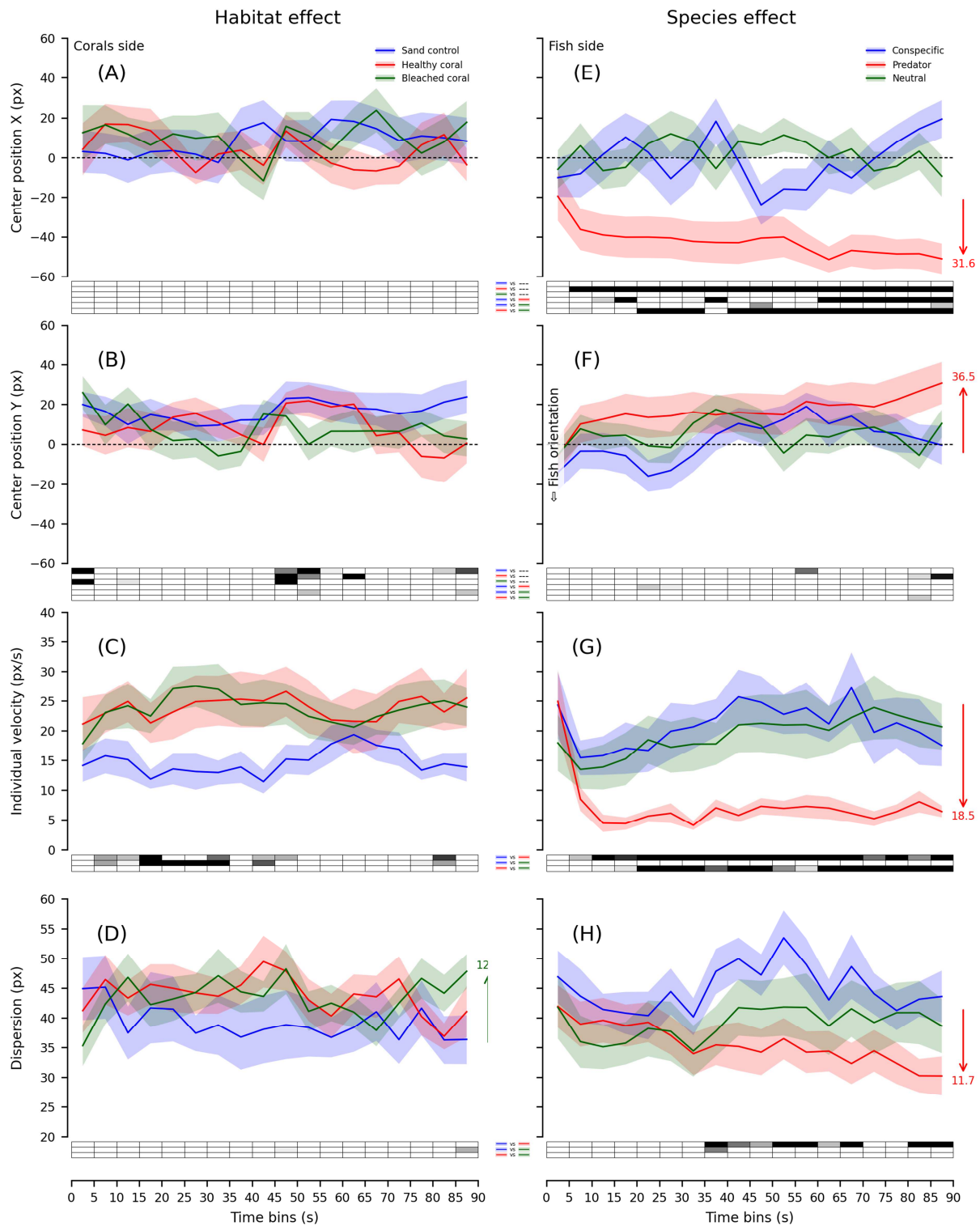
**Links to videos:**

779

×3 (30s): <https://amubox.univ-amu.fr/s/C5KfGMSD7mcWfR9>

780

×6 (15s): <https://amubox.univ-amu.fr/s/oiaKRwAAqRdeWXw>



781

782

783

784

785

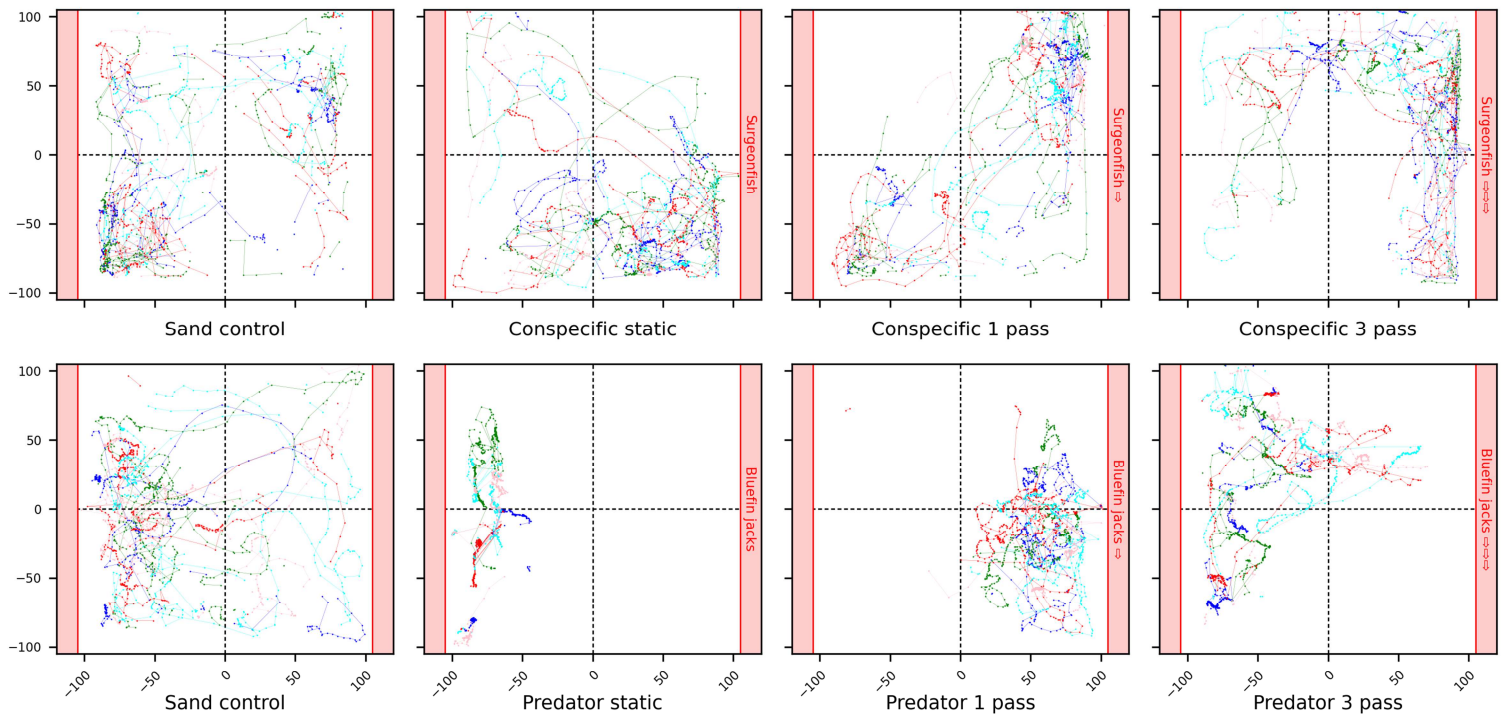
786

787

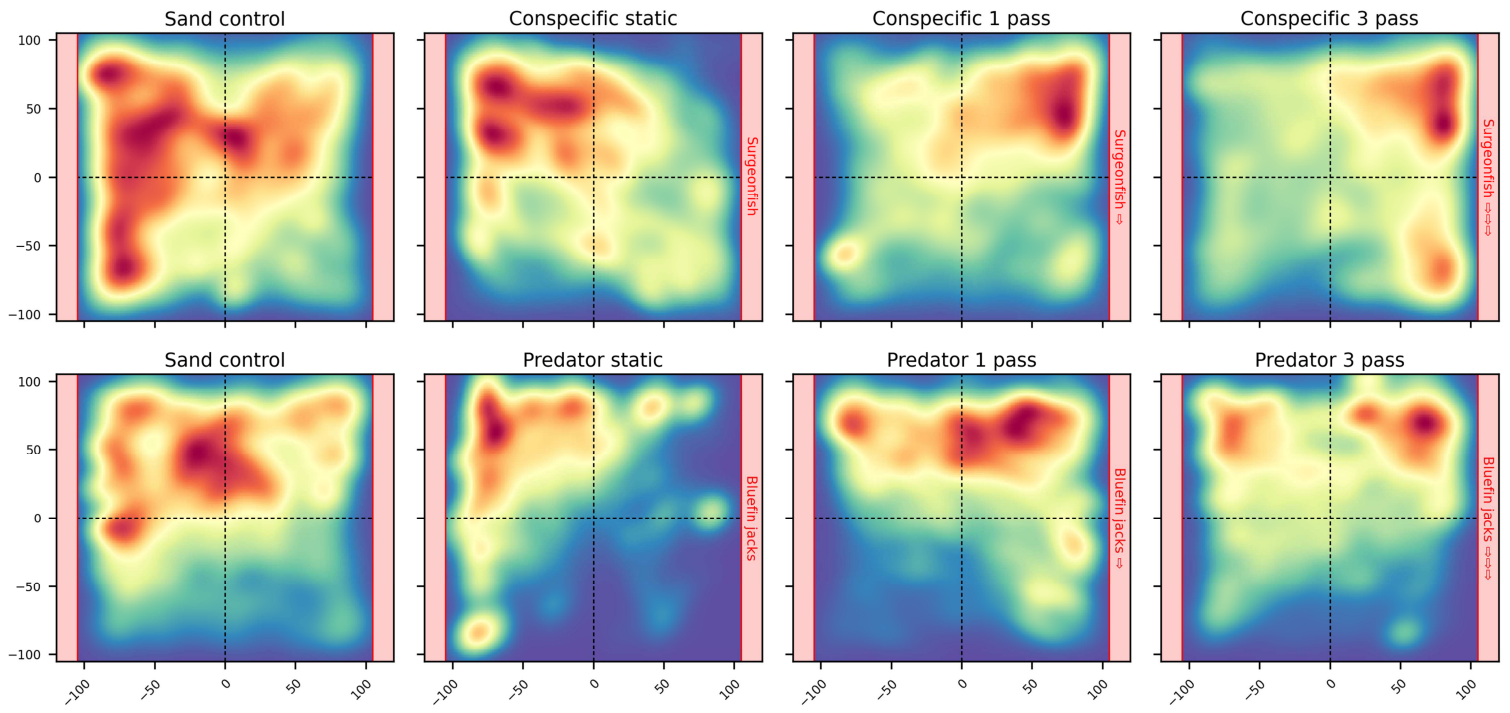
**Fig A5.** Experiment 1 group time series and statistics. X- and Y-positions of the group centre, individual velocity, and group dispersion plotted in time-bins of 5 seconds for the Habitat effect (A-D) and the Species effect (E-H). For each 5-second time-bin, average performance in the conditions was compared to each other or to zero with paired and single-value Student t-tests. Significance level is provided in the boxes below the plots (ranging from light grey for  $P < 0.05/1$  to black for  $P < 0.05/n_{\text{Tests}}$  using Bonferroni's correction for  $n_{\text{Tests}}=3$ ; white for  $P > 0.05$ ).

	Habitat effect				Species effect			
	Condition	Best model	Parameters	RMSE	Condition	Best model	Parameters	RMSE
X-position	Sand control	Quadratic	$a=-0.004$ $b=0.489$ $c=-3.445$	5.59	Conspecific	Quadratic	$a=0.008$ $b=-0.581$ $c=4.006$	11.42
	Healthy coral	Linear	$a=-0.132$ $b=9.209$	9.13	Predator	Exponential	$s=-3.506$ $l=-45.064$ $k=0.172$	3.93
	Bleached coral	Quadratic	$a=0.005$ $b=-0.389$ $c=14.843$	8.51	Neutral	Quadratic	$a=-0.007$ $b=0.627$ $c=-6.574$	7.40
Y-position	Sand control	Linear	$a=0.081$ $b=12.659$	4.78	Conspecific	Quadratic	$a=-0.007$ $b=0.881$ $c=-18.470$	7.41
	Healthy coral	Quadratic	$a=-0.008$ $b=0.627$ $c=1.228$	7.99	Predator	Linear	$a=0.238$ $b=5.842$	4.57
	Bleached coral	Exponential	$s=33.413$ $l=5.127$ $k=0.142$	6.84	Neutral	Linear	$a=0.025$ $b=3.738$	7.20
Velocity	Sand control	Linear	$a=0.025$ $b=13.637$	2.66	Conspecific	Quadratic	$a=-0.002$ $b=0.252$ $c=16.156$	3.78
	Healthy coral	Linear	$a=0.016$ $b=23.210$	3.24	Predator	Exponential	$s=42.560$ $l=6.096$ $k=0.301$	1.94
	Bleached coral	Exponential	$s=15.511$ $l=24.201$ $k=0.203$	2.88	Neutral	Linear	$a=0.095$ $b=14.962$	2.77
Dispersion	Sand control	Exponential	$s=46.648$ $l=38.060$ $k=0.080$	3.01	Conspecific	Quadratic	$a=-0.002$ $b=0.212$ $c=41.197$	3.91
	Healthy coral	Quadratic	$a=-0.002$ $b=0.173$ $c=42.461$	3.33	Predator	Linear	$a=-0.117$ $b=40.813$	1.72
	Bleached coral	Exponential	$s=31.970$ $l=44.103$ $k=0.217$	3.90	Neutral	Linear	$a=0.047$ $b=36.909$	3.02

788 **Table A6.** Experiment 1 best behavioural model fitting. The best model, parameters and corrected RMSE  
789 for each of the 6 conditions and each of the 4 behavioural measures. For each fit, we assessed the  
790 quality of fits computing a RMSE distribution by fitting 1000 times data with shuffled time-bins. Two  
791 quality criteria were used:  $RMSE < dCI(1\%)$  and  $RMSE+20\% < RMSE_{mean}$ . Fits highlighted in red didn't  
792 meet the quality criteria.



793 **Fig A7.** Example of individual trajectories reconstruction in Experiment 2. Individual fish trajectories  
 794 illustrating behavioural reactions of a typical group to the 8 stimuli presented on the aquarium sides  
 795 (red shaded areas) of Experiment 2. The validated positions of fish are connected by coloured lines using  
 796 a minimal distance heuristic to track individual fish in successive frames.

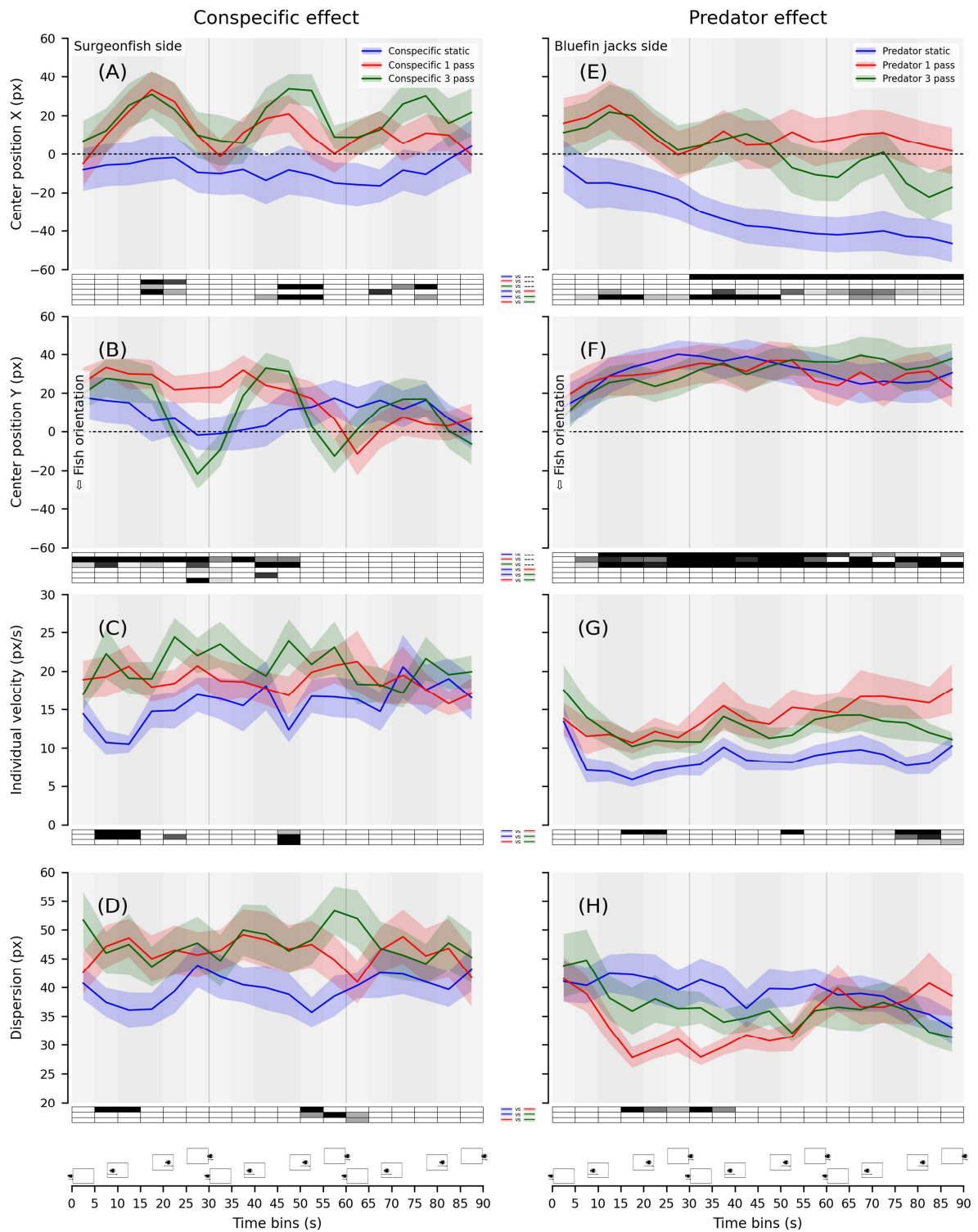


797 **Video A8.** Animation showing the average behavioural responses of Experiment 2. Heatmaps for each  
 798 condition where fish position density in the aquarium is plotted in successive intervals of 1 second.  
 799 Density ranges from low (dark blue) to high (dark red).

800 **Links to videos:**

801 ×3 (30s): <https://amubox.univ-amu.fr/s/F3TWSJoK2PYmP8y>

802 ×6 (15s): <https://amubox.univ-amu.fr/s/oNojasWfoS6j8K5>



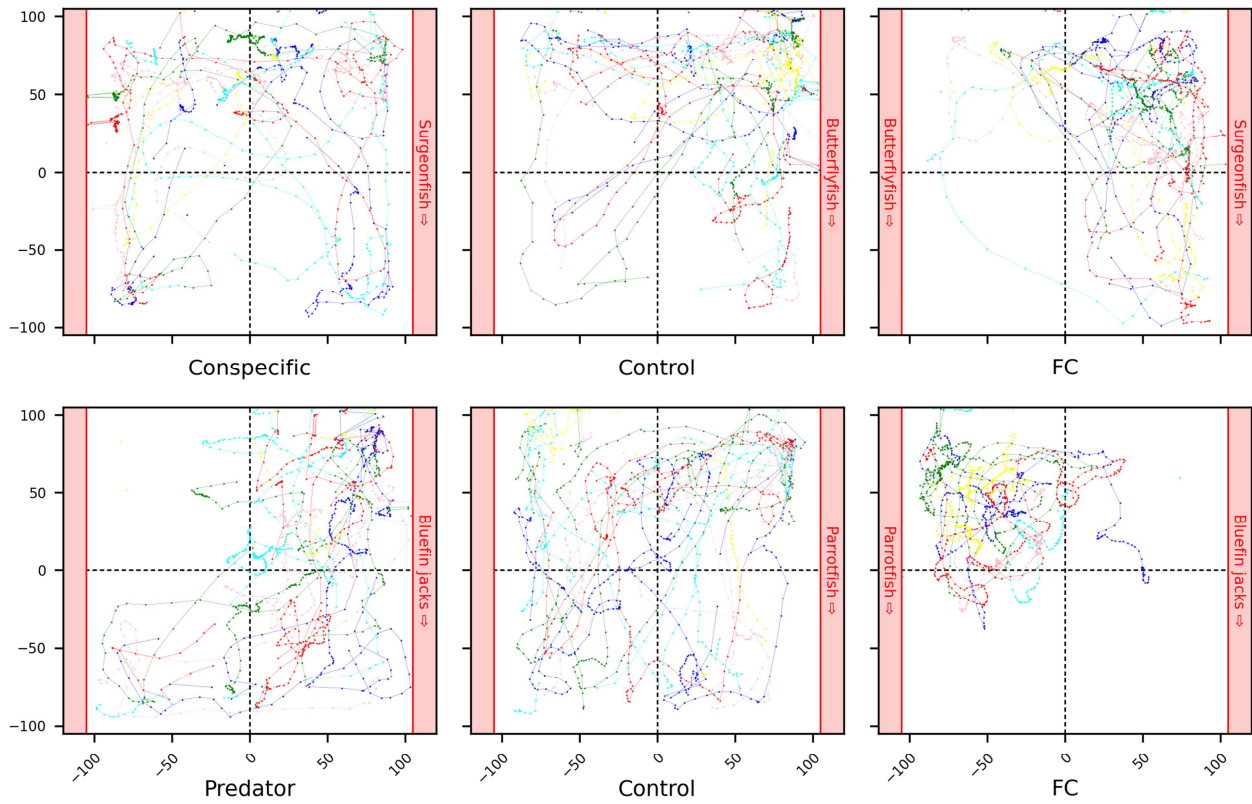
803  
 804  
 805  
 806  
 807  
 808  
 809  
 810

**Fig A9.** Experiment 2 group time series and statistics. X- and Y-positions of the group centre, individual velocity, and group dispersion plotted in time-bins of 5 seconds for the Conspecific effect (A-D) and the Predator effect (E-H). For each 5-second time-bin, average performance in the conditions was compared to each other or to zero with paired and single-value Student t-tests. Significance level is provided in the boxes below the plots (ranging from light grey for  $P < 0.05/1$  to black for  $P < 0.05/n_{\text{Tests}}$  using Bonferroni's correction for  $n_{\text{Tests}}=3$ ; white for  $P > 0.05$ ). Shaded areas highlight the stimuli critical periods based on the on-going distance of the passing virtual shoals in the 3-pass conditions (30 s periodicity).



	Conspecific effect				Predator effect			
	Condition	Best model	Parameters	RMSE	Condition	Best model	Parameters	RMSE
X-position	Conspecific static	Quadratic	$a=0.005$ $b=-0.492$ $c=-0.336$	4.94	Predator static	Quadratic	$a=0.006$ $b=-0.957$ $c=-4.335$	2.42
	Conspecific 1 pass	Linear periodic	$a=-0.131$ $b=17.240$ $A=10.792$ $t_0=13.197$	7.05	Predator 1 pass	Exponential periodic	$s=22.873$ $l=6.347$ $k=0.057$ $A=4.743$ $t_0=17.323$	4.37
	Conspecific 3 pass	Linear periodic	$a=0.020$ $b=17.755$ $A=12.337$ $t_0=12.368$	5.20	Predator 3 pass	Linear periodic	$a=-0.404$ $b=19.353$ $A=7.300$ $t_0=17.241$	3.93
Y-position	Conspecific static	Exponential	$s=24.604$ $l=8.093$ $k=0.159$	6.57	Predator static	Quadratic	$a=-0.009$ $b=0.792$ $c=18.338$	5.00
	Conspecific 1 pass	Linear periodic	$a=-0.399$ $b=34.457$ $A=4.243$ $t_0=14.416$	7.08	Predator 1 pass	Quadratic periodic	$a=-0.006$ $b=0.515$ $c=21.644$ $A=2.372$ $t_0=10.932$	3.88
	Conspecific 3 pass	Exponential periodic	$s=44.447$ $l=7.666$ $k=0.177$ $A=20.884$ $t_0=16.758$	6.63	Predator 3 pass	Exponential periodic	$s=6.331$ $l=36.362$ $k=0.058$ <b><math>A=0.000</math> <math>t_0=0.000</math></b>	3.28
Velocity	Conspecific static	Linear	$a=-0.064$ $b=12.814$	2.79	Predator static	Exponential	$s=21.299$ $l=8.257$ $k=0.497$	1.56
	Conspecific 1 pass	Linear periodic	$a=-0.015$ $b=19.439$ <b><math>A=0.704</math> <math>t_0=26.117</math></b>	2.51	Predator 1 pass	Linear periodic	$a=0.073$ $b=10.845$ <b><math>A=0.752</math> <math>t_0=24.805</math></b>	1.98
	Conspecific 3 pass	Quadratic periodic	$a=-0.002$ $b=0.115$ $c=19.511$ $A=1.497$ $t_0=5.857$	2.53	Predator 3 pass	Exponential periodic	$s=19.405$ $l=12.386$ $k=0.269$ $A=1.302$ $t_0=23.524$	2.00
Dispersion	Conspecific static	Linear	$a=0.036$ $b=38.272$	2.90	Predator static	Quadratic	$a=-0.001$ $b=0.038$ $c=40.885$	1.63
	Conspecific 1 pass	Linear periodic	$a=-0.011$ $b=46.519$ $A=2.033$ $t_0=16.082$	2.66	Predator 1 pass	Quadratic periodic	$a=0.005$ $b=-0.350$ $c=37.443$ $A=2.112$ $t_0=25.626$	3.20
	Conspecific 3 pass	Linear periodic	$a=-0.003$ $b=47.685$ $A=1.871$ $t_0=28.369$	3.22	Predator 3 pass	Exponential periodic	$s=45.052$ $l=34.639$ $k=0.064$ $A=1.280$ $t_0=22.249$	2.34

811 **Table A10.** Experiment 2 best behavioural model fitting. The best model, parameters and corrected  
812 RMSE for each of the 6 retained conditions and each of the 4 behavioural measures. For each fit, we  
813 assessed the quality of fits computing a RMSE distribution by fitting 1000 times data with shuffled time-  
814 bins. Two quality criteria were used:  $RMSE < dCI(1\%)$  and  $RMSE+20\% < RMSE_{mean}$ . Fits highlighted in  
815 red didn't meet the quality criteria.



816

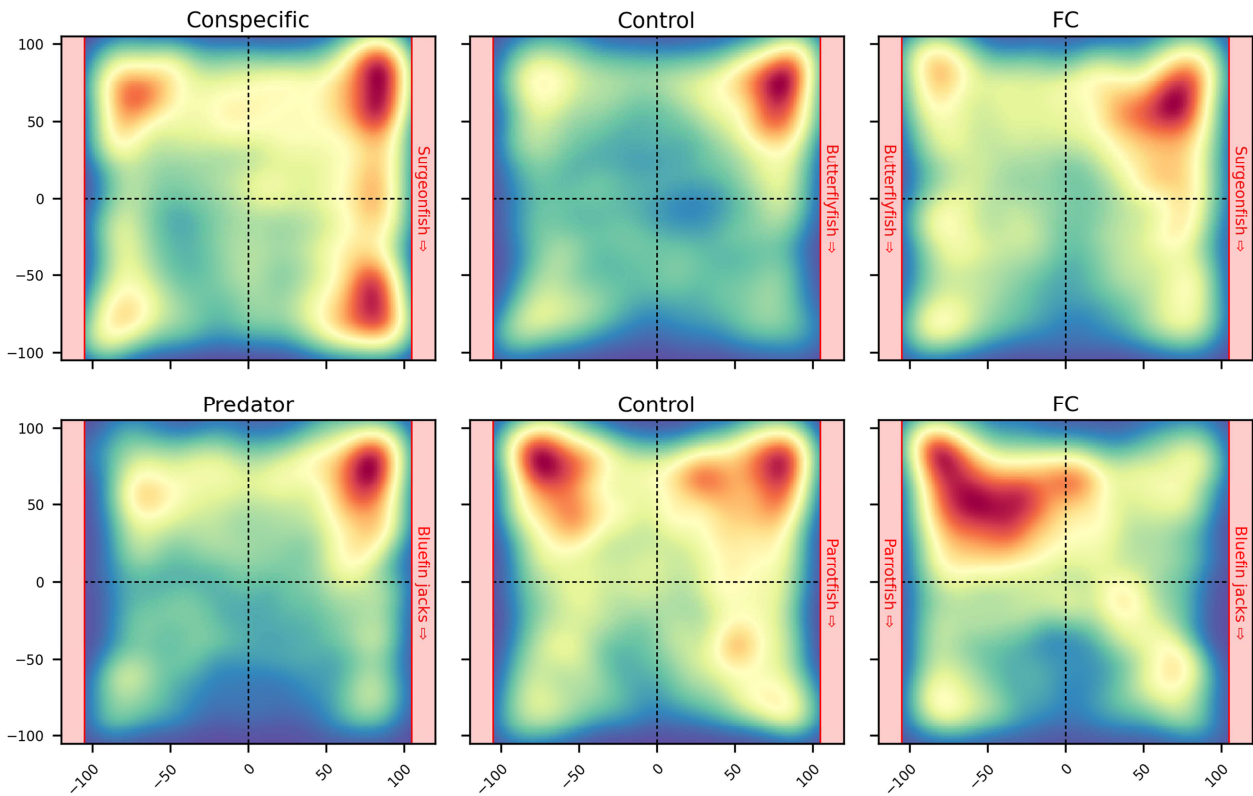
817

818

819

820

**Fig A11.** Example of individual trajectories reconstruction in Experiment 3. Individual fish trajectories illustrating behavioural reactions of a typical group to the 6 stimuli presented on the aquarium sides (red shaded areas) of Experiment 3. The validated positions of fish are connected by coloured lines using a minimal distance heuristic to track individual fish in successive frames.



821

822

**Video A12.** Animation showing the average behavioural responses of Experiment 3. Heatmaps for each condition where fish position density in the aquarium is plotted in successive intervals of 1 second. Density ranges from low (dark blue) to high (dark red).

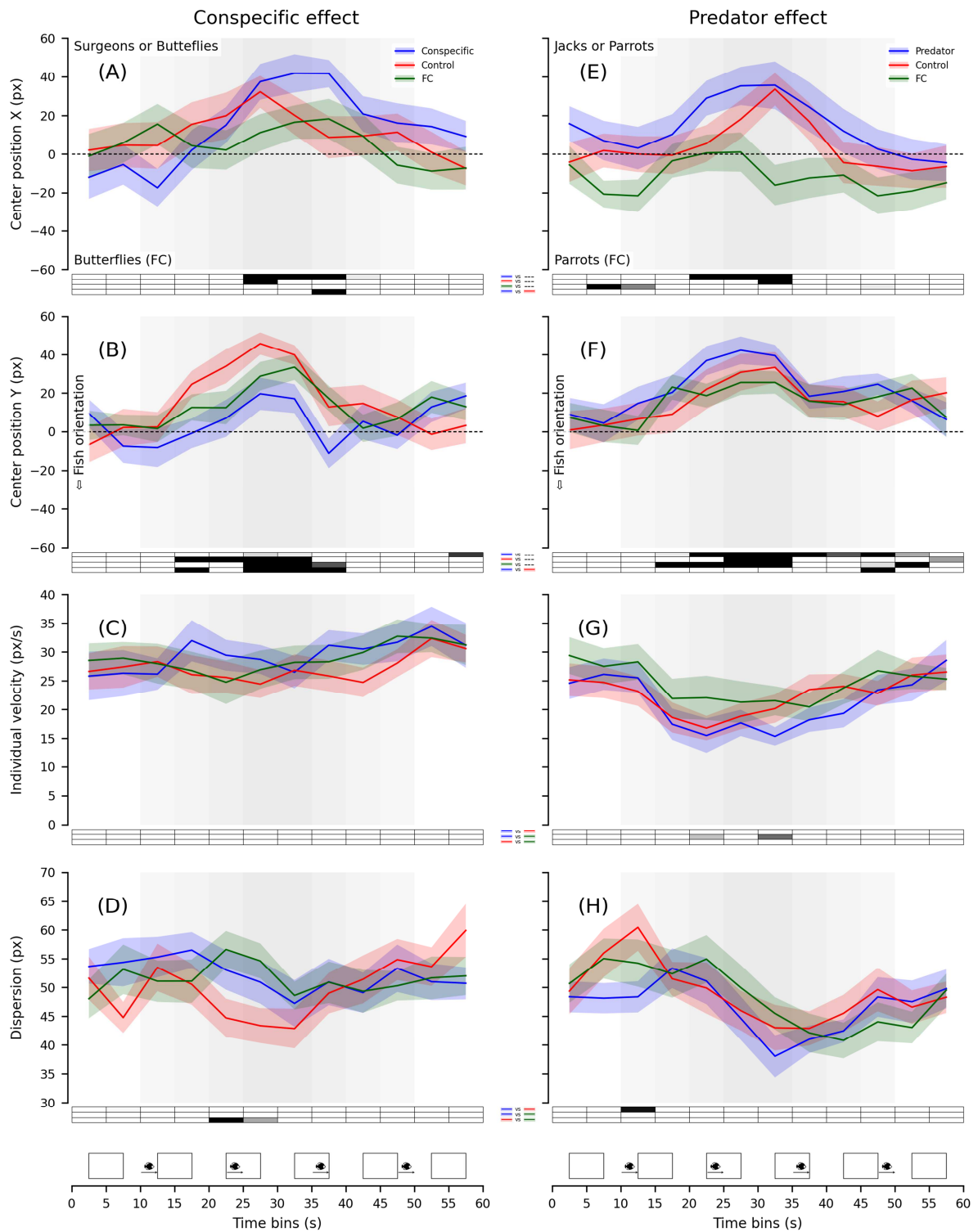
823

824

825 **Links to videos:**

826 ×3 (20s): <https://amubox.univ-amu.fr/s/32EN2ox6temcaeM>

827 ×6 (10s): <https://amubox.univ-amu.fr/s/6Zq322jsciYDwka>



828

829

830

831

832

833

834

835

**Fig A13.** Experiment 3 group time series and statistics. X- and Y-positions of the group centre, individual velocity, and group dispersion plotted in time-bins of 5 seconds for the Conspecific effect (A-D) and the Predator effect (E-H). For each 5-second time-bin, average performance in the conditions was compared to each other or to zero with paired and single-value Student t-tests. Significance level is provided in the boxes below the plots (ranging from light grey for  $P < 0.05/1$  to black for  $P < 0.05/n_{\text{Tests}}$  using Bonferroni's correction for  $n_{\text{Tests}}=3$ ; white for  $P > 0.05$ ). Shaded areas highlight the stimuli critical period based on the on-going distance of the passing virtual shoals.

	Conspecific effect				Predator effect			
	Condition	Best model	Parameters	RMSE	Condition	Best model	Parameters	RMSE
X-position	Conspecific	Linear periodic	$a=0.808$ $b=-4.566$ $A=22.852$ $t_0=8.962$	4.26	Predator	Linear periodic	$a=0.019$ $b=18.456$ $A=18.453$ $t_0=10.294$	2.41
	Control	Linear periodic	$a=0.407$ $b=3.059$ $A=13.168$ $t_0=15.348$	4.29	Control	Linear periodic	$a=-0.440$ $b=21.053$ $A=18.382$ $t_0=6.960$	5.71
	FC	Linear periodic	$a=-0.916$ $b=36.477$ $A=16.326$ $t_0=2.082$	3.88	FC	Linear periodic	$a=0.292$ $b=-19.370$ $A=12.545$ $t_0=16.313$	6.54
Y-position	Conspecific	Linear periodic	$a=0.445$ $b=-10.035$ $A=13.061$ $t_0=14.388$	8.80	Predator	Quadratic periodic	$a=0.026$ $b=-1.000$ $c=29.847$ $A=19.427$ $t_0=13.941$	4.29
	Control	Linear periodic	$a=0.426$ $b=9.874$ $A=22.756$ $t_0=13.900$	5.88	Control	Linear periodic	$a=0.128$ $b=13.793$ $A=13.220$ $t_0=10.641$	4.01
	FC	Linear periodic	$a=0.099$ $b=11.310$ $A=14.318$ $t_0=10.886$	5.47	FC	Linear periodic	$a=0.633$ $b=-1.310$ $A=12.229$ $t_0=15.789$	4.36
Velocity	Conspecific	Exponential periodic	$s=-100.0$ $l=30.610$ $k=0.248$ $A=2.306$ $t_0=27.964$	2.60	Predator	Quadratic periodic	$a=0.015$ $b=-1.000$ $c=33.344$ $A=2.584$ $t_0=35.378$	1.95
	Control	Quadratic periodic	$a=0.016$ $b=-1.000$ $c=39.365$ $A=1.311$ $t_0=9.304$	2.30	Control	Linear periodic	$a=-0.091$ $b=23.697$ $A=4.623$ $t_0=37.174$	2.12
	FC	Linear periodic	$a=0.117$ $b=24.698$ $A=1.798$ $t_0=32.692$	2.25	FC	Quadratic periodic	$a=0.016$ $b=-1.000$ $c=36.671$ $A=0.752$ $t_0=34.227$	1.87
Dispersion	Conspecific	Linear periodic	$a=-0.039$ $b=53.221$ $A=3.296$ $t_0=25.351$	2.35	Predator	Quadratic periodic	$a=-0.015$ $b=1.000$ $c=31.155$ $A=9.249$ $t_0=24.507$	2.27
	Control	Linear periodic	$a=0.020$ $b=48.171$ $A=6.079$ $t_0=30.805$	2.80	Control	Quadratic periodic	$a=0.012$ $b=-1.000$ $c=65.723$ $A=3.597$ $t_0=28.083$	1.90
	FC	Linear periodic	$a=0.085$ $b=49.016$ $A=3.720$ $t_0=17.870$	2.61	FC	Linear periodic	$a=-0.123$ $b=51.698$ $A=5.906$ $t_0=20.223$	2.54

836 **Table A14.** Experiment 3 best behavioural model fitting. The best model, parameters and corrected  
837 RMSE for each of the 6 conditions and each of the 4 behavioural measures. For each fit, we assessed the  
838 quality of fits computing a RMSE distribution by fitting 1000 times data with shuffled time-bins. Two  
839 quality criteria were used:  $RMSE < dCI(1\%)$  and  $RMSE+20\% < RMSE_{mean}$ . Fits highlighted in red didn't  
840 meet the quality criteria.

## 841 Data availability

842 Raw data files, global plots (all groups), and individual plots (trajectories, position scatter  
843 plots, animated position density maps, grouped bin data) and the Python code used for data  
844 processing for each experiment can be found in the following public repository:

845 <https://amubox.univ-amu.fr/s/WyYRBirn3pmz0qT>

## 846 Acknowledgements

847 We would like to thank the technical staff of the CRIOBE for their support, and in particular  
848 Matthieu Reynaud for capturing the larvae used in the experiments. This work received support from  
849 the French government under the France 2030 investment plan, as part of the Initiative d'Excellence  
850 d'Aix-Marseille Université – A\*MIDEX, from the Fondation de France (2019-08602), from the Office

851 Français de la Biodiversité (AFB/2019/385 – OFB.20.0888), and from the Agence Nationale de la  
852 Recherche (ANR-19-CE34-0006-Manini and ANR-19-CE14-0010-SENSO).

## 853 References

- 854 Alatalo, R. V., Höglund, J., & Lundberg, A. (1991). Lekking in the black grouse—A test of male viability. *Nature*,  
855 352(6331), 155–156.
- 856 Atema, J., Kingsford, M. J., & Gerlach, G. (2002). Larval reef fish could use odour for detection, retention and  
857 orientation to reefs. *Marine Ecology Progress Series*, 241, 151–160.  
858 <https://doi.org/10.3354/meps241151>
- 859 Baldauf, S. A., Kullmann, H., Thünken, T., Winter, S., & Bakker, T. C. M. (2009). Computer animation as a tool to  
860 study preferences in the cichlid *Pelvicachromis taeniatus*. *Journal of Fish Biology*, 75(3), 738–746.  
861 <https://doi.org/10.1111/j.1095-8649.2009.02347.x>
- 862 Barker, A. J., & Baier, H. (2015). Sensorimotor decision making in the zebrafish tectum. *Current Biology: CB*,  
863 25(21), 2804–2814. <https://doi.org/10.1016/j.cub.2015.09.055>
- 864 Barth, P., Berenshtein, I., Besson, M., Roux, N., Parmentier, E., Banaigs, B., & Lecchini, D. (2015). From the  
865 ocean to a reef habitat: How do the larvae of coral reef fishes find their way home? A state of art on the  
866 latest advances. *Vie Milieu*, 10.
- 867 Beldade, R., Blandin, A., O'Donnell, R., & Mills, S. C. (2017). Cascading effects of thermally-induced anemone  
868 bleaching on associated anemonefish hormonal stress response and reproduction. *Nature*  
869 *Communications*, 8(1), 716. <https://doi.org/10.1038/s41467-017-00565-w>
- 870 Beldade, R., Holbrook, S. J., Schmitt, R. J., Planes, S., & Bernardi, G. (2016). Spatial patterns of self-recruitment  
871 of a coral reef fish in relation to island-scale retention mechanisms. *Molecular Ecology*, 25(20), 5203–  
872 5211.
- 873 Beldade, R., Holbrook, S. J., Schmitt, R. J., Planes, S., Malone, D., & Bernardi, G. (2012). Larger female fish  
874 contribute disproportionately more to self-replenishment. *Proceedings of the Royal Society B: Biological*  
875 *Sciences*, 279(1736), 2116–2121.
- 876 Besson, M., Feeney, W. E., Moniz, I., François, L., Brooker, R. M., Holzer, G., Metian, M., Roux, N., Laudet, V., &  
877 Lecchini, D. (2020). Anthropogenic stressors impact fish sensory development and survival via thyroid  
878 disruption. *Nature Communications*, 11(1), 3614. <https://doi.org/10.1038/s41467-020-17450-8>
- 879 Besson, M., Gache, C., Bertucci, F., Brooker, R. M., Roux, N., Jacob, H., Berthe, C., Sovrano, V. A., Dixson, D. L., &  
880 Lecchini, D. (2017). Exposure to agricultural pesticide impairs visual lateralization in a larval coral reef  
881 fish. *Scientific Reports*, 7(1), Article 1. <https://doi.org/10.1038/s41598-017-09381-0>
- 882 Booth, D. J. (1992). Larval settlement patterns and preferences by domino damselfish *Dascyllus albisella* Gill.  
883 *Journal of Experimental Marine Biology and Ecology*, 155(1), 85–104.
- 884 Brookes, J., Warburton, M., Alghadier, M., Mon-Williams, M., & Mushtaq, F. (2020). Studying human behavior  
885 with virtual reality: The Unity Experiment Framework. *Behavior Research Methods*, 52(2), 455–463.  
886 <https://doi.org/10.3758/s13428-019-01242-0>
- 887 Carmichael, L. (1952). The Study of Instinct. N. Tinbergen. New York: Oxford Univ. Press, 1951. 228 pp. \$7.00.  
888 *Science*, 115(2990), 438–439.

889 Coppock, A. G., Gardiner, N. M., & Jones, G. P. (2013). Olfactory discrimination in juvenile coral reef fishes:  
890 Response to conspecifics and corals. *Journal of Experimental Marine Biology and Ecology*, *443*, 21–26.  
891 <https://doi.org/10.1016/j.jembe.2013.02.026>

892 Doherty, P. J. (2002). CHAPTER 15—Variable Replenishment and the Dynamics of Reef Fish Populations. In P. F.  
893 Sale (Ed.), *Coral Reef Fishes* (pp. 327–355). Academic Press. [https://doi.org/10.1016/B978-012615185-](https://doi.org/10.1016/B978-012615185-5/50019-0)  
894 [5/50019-0](https://doi.org/10.1016/B978-012615185-5/50019-0)

895 Drew, L. (2019). The mouse in the video game. *Nature*, *567*, 158. <https://doi.org/10.1038/d41586-019-00791-w>

896 Dunn, T. W., Gebhardt, C., Naumann, E. A., Riegler, C., Ahrens, M. B., Engert, F., & Del Bene, F. (2016). Neural  
897 Circuits Underlying Visually Evoked Escapes in Larval Zebrafish. *Neuron*, *89*(3), 613–628.  
898 <https://doi.org/10.1016/j.neuron.2015.12.021>

899 Harpaz, R., Nguyen, M. N., Bahl, A., & Engert, F. (2021). Precise visuomotor transformations underlying  
900 collective behavior in larval zebrafish. *Nature Communications*, *12*(1), Article 1.  
901 <https://doi.org/10.1038/s41467-021-26748-0>

902 Harvey, C. D., Collman, F., Dombeck, D. A., & Tank, D. W. (2009). Intracellular dynamics of hippocampal place  
903 cells during virtual navigation. *Nature*, *461*(7266), Article 7266. <https://doi.org/10.1038/nature08499>

904 Holles, S., Simpson, S. D., Radford, A. N., Berten, L., & Lecchini, D. (2013). Boat noise disrupts orientation  
905 behaviour in a coral reef fish. *Marine Ecology Progress Series*, *485*, 295–300.  
906 <https://doi.org/10.3354/meps10346>

907 Holzer, G., Besson, M., Lambert, A., François, L., Barth, P., Gillet, B., Hughes, S., Piganeau, G., Leulier, F., Viriot,  
908 L., Lecchini, D., & Laudet, V. (2017). Fish larval recruitment to reefs is a thyroid hormone-mediated  
909 metamorphosis sensitive to the pesticide chlorpyrifos. *ELife*, *6*, e27595.  
910 <https://doi.org/10.7554/eLife.27595>

911 Huang, K.-H., Rupprecht, P., Frank, T., Kawakami, K., Bouwmeester, T., & Friedrich, R. W. (2020). A virtual  
912 reality system to analyze neural activity and behavior in adult zebrafish. *Nature Methods*, *17*(3), Article  
913 3. <https://doi.org/10.1038/s41592-020-0759-2>

914 Huijbers, C. M., Nagelkerken, I., Lössbroek, P. A. C., Schulten, I. E., Siegenthaler, A., Holderied, M. W., &  
915 Simpson, S. D. (2012). A test of the senses: Fish select novel habitats by responding to multiple cues.  
916 *Ecology*, *93*(1), 46–55. <https://doi.org/10.1890/10-2236.1>

917 Ioannou, C. C., Guttal, V., & Couzin, I. D. (2012). Predatory Fish Select for Coordinated Collective Motion in  
918 Virtual Prey. *Science*, *337*(6099), 1212–1215. <https://doi.org/10.1126/science.1218919>

919 Katzir, G. (1981). Visual aspects of species recognition in the damselfish *Dascyllus aruanus* L. (Pisces,  
920 Pomacentridae). *Animal Behaviour*, *29*(3), 842–849. [https://doi.org/10.1016/S0003-3472\(81\)80019-X](https://doi.org/10.1016/S0003-3472(81)80019-X)

921 Künzler, R., & Bakker, T. (1998). Computer Animations as a Tool in the Study of Mating Preferences. *Behaviour*,  
922 *135*(8), 1137–1159. <https://doi.org/10.1163/156853998792913537>

923 Lara, M. R. (2001). Morphology of the eye and visual acuities in the settlement-intervals of some Coral Reef  
924 Fishes (Labridae, Scaridae). *Environmental Biology of Fishes*, *62*(4), 365–378.  
925 <https://doi.org/10.1023/A:1012214229164>

926 Larsch, J., & Baier, H. (2018). Biological Motion as an Innate Perceptual Mechanism Driving Social Affiliation.  
927 *Current Biology: CB*, *28*(22), 3523–3532.e4. <https://doi.org/10.1016/j.cub.2018.09.014>

928 Lecchini, D., & Galzin, R. (2003). Influence of pelagic and benthic, biotic and abiotic, stochastic and  
929 deterministic processes on the dynamics of auto-recruitment of coral reef fish: A review. *Cybium*, *27*,  
930 167–184.

931 Lecchini, D., Peyrusse, K., Lanyon, R. G., & Lecellier, G. (2014). Importance of visual cues of conspecifics and  
932 predators during the habitat selection of coral reef fish larvae. *Comptes Rendus Biologies*, 337(5), 345–  
933 351. <https://doi.org/10.1016/j.crvi.2014.03.007>

934 Lecchini, D., Shima, J., Banaigs, B., & Galzin, R. (2005). Larval sensory abilities and mechanisms of habitat  
935 selection of a coral reef fish during settlement. *Oecologia*, 143(2), 326–334.  
936 <https://doi.org/10.1007/s00442-004-1805-y>

937 Lecchini, D., Waqalevu, V. P., Parmentier, E., Radford, C. A., & Banaigs, B. (2013). Fish larvae prefer coral over  
938 algal water cues: Implications of coral reef degradation. *Marine Ecology Progress Series*, 475, 303–307.  
939 <https://doi.org/10.3354/meps10094>

940 Leis, J. M. (2015). 23 Is dispersal of larval reef fishes passive? *Ecology of Fishes on Coral Reefs*, 223.

941 Leis, J. M., & Carson-Ewart, B. M. (1999). In situ swimming and settlement behaviour of larvae of an Indo-  
942 Pacific coral-reef fish, the coral trout *Plectropomus leopardus* (Pisces: Serranidae). *Marine Biology*,  
943 134(1), 51–64. <https://doi.org/10.1007/s002270050524>

944 Leis, J. M., & McCormick, M. I. (2002). CHAPTER 8—The Biology, Behavior, and Ecology of the Pelagic, Larval  
945 Stage of Coral Reef Fishes. In P. F. Sale (Ed.), *Coral Reef Fishes* (pp. 171–199). Academic Press.  
946 <https://doi.org/10.1016/B978-012615185-5/50011-6>

947 Losey, G. S., McFarland, W. N., Loew, E. R., Zamzow, J. P., Nelson, P. A., & Marshall, N. J. (2003). Visual Biology  
948 of Hawaiian Coral Reef Fishes. I. Ocular Transmission and Visual Pigments. *Copeia*, 2003(3), 433–454.

949 McCormick, M. I., Makey, L., & Dufour, V. (2002). Comparative study of metamorphosis in tropical reef fishes.  
950 *Marine Biology*, 141(5), 841–853.

951 Mills, S. C., Alatalo, R. V., Koskela, E., Mappes, J., Mappes, T., & Oksanen, T. A. (2007). Signal reliability  
952 compromised by genotype-by-environment interaction and potential mechanisms for its preservation.  
953 *Evolution; International Journal of Organic Evolution*, 61(7), 1748–1757. [https://doi.org/10.1111/j.1558-  
954 5646.2007.00145.x](https://doi.org/10.1111/j.1558-5646.2007.00145.x)

955 Mills, S. C., Beldade, R., Henry, L., Laverty, D., Nedelec, S. L., Simpson, S. D., & Radford, A. N. (2020). Hormonal  
956 and behavioural effects of motorboat noise on wild coral reef fish. *Environmental Pollution (Barking,  
957 Essex: 1987)*, 262, 114250. <https://doi.org/10.1016/j.envpol.2020.114250>

958 Montgomery, J. C., Jeffs, A., Simpson, S. D., Meekan, M., & Tindle, C. (2006). Sound as an orientation cue for  
959 the pelagic larvae of reef fishes and decapod crustaceans. *Advances in Marine Biology*, 51, 143–196.  
960 [https://doi.org/10.1016/S0065-2881\(06\)51003-X](https://doi.org/10.1016/S0065-2881(06)51003-X)

961 Mossio, M., Vidal, M., & Berthoz, A. (2008). Traveled distances: New insights into the role of optic flow. *Vision  
962 Res.*, 48(2), 289–303.

963 Myrberg, A. A., & Fuiman, L. A. (2002). The sensory world of coral reef fishes. *Coral Reef Fishes: Dynamics and  
964 Diversity in a Complex Ecosystem*, 123–148.

965 Nanninga, G. B., Côté, I. M., Beldade, R., & Mills, S. C. (2017). Behavioural acclimation to cameras and observers  
966 in coral reef fishes. *Ethology*, 123(10), 705–711. <https://doi.org/10.1111/eth.12642>

967 Nedelec, S. L., Mills, S. C., Radford, A. N., Beldade, R., Simpson, S. D., Nedelec, B., & Côté, I. M. (2017).  
968 Motorboat noise disrupts co-operative interspecific interactions. *Scientific Reports*, 7(1), 6987.  
969 <https://doi.org/10.1038/s41598-017-06515-2>

970 Neri, P. (2012). Feature binding in zebrafish. *Animal Behaviour*, 84(2), 485–493.  
971 <https://doi.org/10.1016/j.anbehav.2012.06.005>



972 Parmentier, E., Berten, L., Rigo, P., Aubrun, F., Nedelec, S. L., Simpson, S. D., & Lecchini, D. (2015). The influence  
973 of various reef sounds on coral-fish larvae behaviour. *Journal of Fish Biology*, *86*(5), 1507–1518.  
974 <https://doi.org/10.1111/jfb.12651>

975 Portugues, R., & Engert, F. (2009). The neural basis of visual behaviors in the larval zebrafish. *Current Opinion in*  
976 *Neurobiology*, *19*(6), 644–647. <https://doi.org/10.1016/j.conb.2009.10.007>

977 Rosenthal, G. G., & Evans, C. S. (1998). Female preference for swords in *Xiphophorus helleri* reflects a bias for  
978 large apparent size. *Proceedings of the National Academy of Sciences of the United States of America*,  
979 *95*(8), 4431–4436. <https://doi.org/10.1073/pnas.95.8.4431>

980 Roux, N., Duran, E., Lanyon, R. G., Frédérick, B., Berthe, C., Besson, M., Dixon, D. L., & Lecchini, D. (2016). Brain  
981 lateralization involved in visual recognition of conspecifics in coral reef fish at recruitment. *Animal*  
982 *Behaviour*, *117*, 3–8. <https://doi.org/10.1016/j.anbehav.2016.04.011>

983 Saverino, C., & Gerlai, R. (2008). The social zebrafish: Behavioral responses to conspecific, heterospecific, and  
984 computer animated fish. *Behavioural Brain Research*, *191*(1), 77–87.  
985 <https://doi.org/10.1016/j.bbr.2008.03.013>

986 Schligler, J., Cortese, D., Beldade, R., Swearer, S. E., & Mills, S. C. (2021). Long-term exposure to artificial light at  
987 night in the wild decreases survival and growth of a coral reef fish. *Proceedings. Biological Sciences*,  
988 *288*(1952), 20210454. <https://doi.org/10.1098/rspb.2021.0454>

989 Siu, G., Bacchet, P., Bernardi, G., Brooks, A. J., Carlot, J., Causse, R., Claudet, J., Clua, É., Delrieu-Trottin, E.,  
990 Espiau, B., Harmelin-Vivien, M., Keith, P., Lecchini, D., Madi-Moussa, R., Parravicini, V., Planes, S.,  
991 Ponsonnet, C., Randall, J. E., Sasal, P., ... Galzin, R. (2017). *Shore fishes of French Polynesia*. 34.

992 Stowers, J. R., Hofbauer, M., Bastien, R., Griessner, J., Higgins, P., Farooqui, S., Fischer, R. M., Nowikovskiy, K.,  
993 Haubensak, W., Couzin, I. D., Tessmar-Raible, K., & Straw, A. D. (2017). Virtual reality for freely moving  
994 animals. *Nature Methods*, *14*(10), 995–1002. <https://doi.org/10.1038/nmeth.4399>

995 Tarr, M. J., & Warren, W. H. (2002). Virtual reality in behavioral neuroscience and beyond. *Nat. Neurosci.*, *5*  
996 *Suppl*, 1089–1092.

997 Tettamanti, V., de Busserolles, F., Lecchini, D., Marshall, N. J., & Cortesi, F. (2019). Visual system development  
998 of the spotted unicornfish, *Naso brevirostris* (Acanthuridae). *Journal of Experimental Biology*, *222*(24),  
999 jeb209916. <https://doi.org/10.1242/jeb.209916>

1000 Tolimieri, N., Haine, O., Jeffs, A., McCauley, R., & Montgomery, J. (2004). Directional orientation of  
1001 pomacentrid larvae to ambient reef sound. *Coral Reefs*, *23*(2), 184–191.  
1002 <https://doi.org/10.1007/s00338-004-0383-0>

1003 Vail, A. L., & McCormick, M. I. (2011). Metamorphosing reef fishes avoid predator scent when choosing a  
1004 home. *Biology Letters*, *7*(6), 921–924. <https://doi.org/10.1098/rsbl.2011.0380>

1005 Vidal, M., Amorim, M.-A., & Berthoz, A. (2004). Navigating in a virtual three-dimensional maze: How do  
1006 egocentric and allocentric reference frames interact? *Cognitive Brain Research*, *19*(3), 244–258.

1007 Vidal, M., & Bühlhoff, H. H. (2009). Storing upright turns: How visual and vestibular cues interact during the  
1008 encoding and recalling process. *Experimental Brain Research*, *200*(1), 37–49.  
1009 <https://doi.org/10.1007/s00221-009-1980-5>

1010 Vidal, M., Lehmann, A., & Bühlhoff, H. H. (2009). A multisensory approach to spatial updating: The case of  
1011 mental rotations. *Experimental Brain Research*, *197*(1), 59–68. [https://doi.org/10.1007/s00221-009-](https://doi.org/10.1007/s00221-009-1892-4)  
1012 [1892-4](https://doi.org/10.1007/s00221-009-1892-4)